

Development of a modelling methodology for simulation of long-term morphological evolution of the southern Baltic coast

Wenyan Zhang · Jan Harff · Ralf Schneider ·
Chaoyu Wu

Received: 14 December 2009 / Accepted: 15 June 2010 / Published online: 29 June 2010
© Springer-Verlag 2010

Abstract The Darss–Zingst peninsula at the southern Baltic Sea is a typical wave-dominated barrier island system which includes an outer barrier island and an inner lagoon. The formation of the Darss–Zingst peninsula dates back to the Littorina Transgression onset about 8,000 cal BP. It originated from several discrete islands, has been reshaped by littoral currents, wind-induced waves during the last 8,000 years and evolved into a complex barrier island system as today; thus, it may serve as an example to study the coastal evolution under long-term climate change. A methodology for developing a long-term (decadal-to-centennial) process-based morphodynamic model for the southern Baltic coastal environment is presented here. The methodology consists of two main components: (1) a preliminary analysis of the key processes driving the morphological evolution of the study area based on statistical analysis of meteorological data and sensitivity studies; (2) a multi-scale high-resolution process-based

model. The process-based model is structured into eight main modules. The two-dimensional vertically integrated circulation module, the wave module, the bottom boundary layer module, the sediment transport module, the cliff erosion module and the nearshore storm module are real-time calculation modules which aim at solving the short-term processes. A bathymetry update module and a long-term control function set, in which the ‘reduction’ concepts and technique for morphological update acceleration are implemented, are integrated to up-scale the effects of short-term processes to a decadal-to-centennial scale. A series of multi-scale modelling strategies are implemented in the application of the model to the research area. Successful hindcast of the coastline change of the Darss–Zingst peninsula for the last 300 years validates the modelling methodology. Model results indicate that the coastline change of the Darss–Zingst peninsula is dominated by mechanisms acting on different time scales. The coastlines of Darss and the island of Hiddensee are mainly reshaped by long-term effects of waves and longshore currents, while the coastline change of the Zingst peninsula is due to a combination of long-term effects of waves and short-term effects caused by wind storms.

Responsible Editor: Birgit Andrea Klein

W. Zhang (✉) · C. Wu
Center for Coastal Ocean Science and Technology Research,
Zhongshan University,
510275 Guangzhou, China
e-mail: wzhang@ipp.mpg.de

J. Harff
Baltic Sea Research Institute Warnemuende,
University of Rostock,
Seestrasse 15a,
18119 Rostock, Germany

R. Schneider
Max-Planck-Institute for Plasma Physics,
Wendelsteinstrasse 1,
17491 Greifswald, Germany

Keywords Multi-scale · Numerical model · Coastal evolution · Wave dominated · Wind analysis

1 Introduction

High-resolution process-based models have proven to be useful tools in helping for further understanding and quantification of mechanisms driving coastal evolution. These models are based on first principles regulating the hydrodynamics and physics of sediment transport, and

utilize state-of-the-art fluid dynamics modelling to solve fluid mechanics equations coupled with rules for sediment transport (Fagherazzi and Overeem 2007). Although the high-resolution process-based models are always reliable in modelling short-term (hourly to daily scale) morphological evolution of coastal and shelf areas, the application of these models to long-term (decadal-to-centennial scale) morphodynamics is severely restricted. This is mainly due to three factors: (1) the time step of calculation in high-resolution process-based models is determined by the shortest time scale process, i.e. usually at the order of seconds or minutes. Numerical schemes used in computer for solving the partial differential equations such as the Navier–Stokes equation inevitably generate truncation errors. Truncation errors generated after each calculation time step can pile up during continuous run cycles in a long-term model and lead to large bias between the final simulation results and the reality, (2) detailed time series of data covering such a long time span serving for model boundary input is absent and (3) the variation of bathymetry occurring in a stochastic short time period, e.g. in a wind storm period, may exceed the change in a longer time span (1 year).

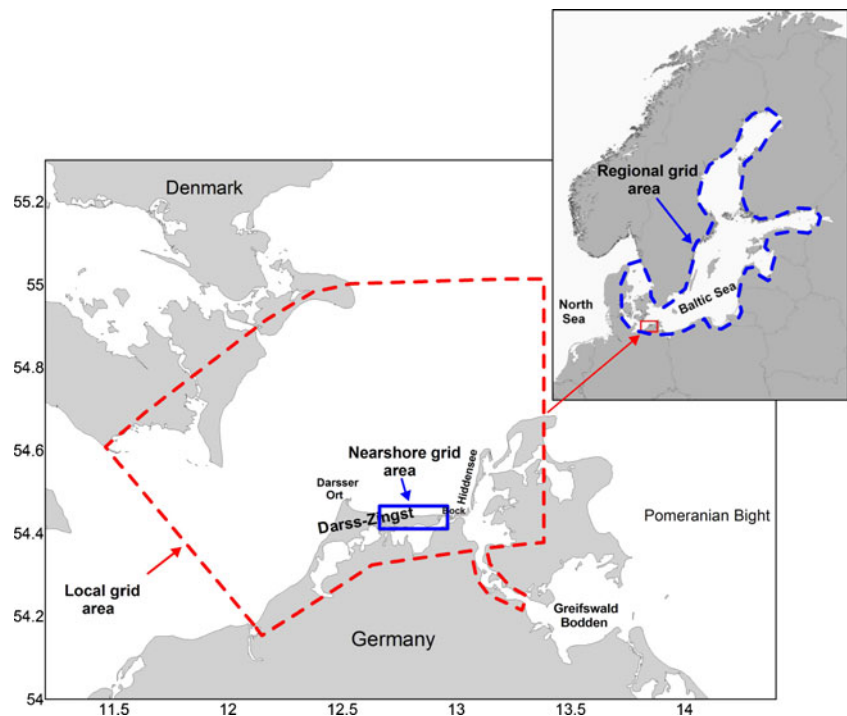
One way of bridging the gap between the simulation of short-term hydrodynamics, sediment transport and morphological changes taking place over much longer timescales is integrating the concepts of ‘reduction’ (de Vriend et al. 1993a, b; Latteux 1995) and techniques of morphological update acceleration (Roelvink 2006; Jones et al. 2007) into the high-resolution process-based models. Three approaches can be concluded according to the ‘reduction’ strategy: (1) model reduction, in which only the main driving terms on the scale of interest are considered, small-scale processes which can be smoothed over a longer time period are omitted or integrated into an average term; (2) input reduction, in which the input data should be refined into some representative data groups which are able to produce similar results as the whole variety of real-time series on the scale of interest; (3) behaviour-based models, in which the small-scale processes are replaced by observational knowledge. By ‘extracting’ the most important processes responsible for the long-term coastal morphological evolution based on the concepts of ‘reduction’ and combining them with the technique of morphological update acceleration, high-resolution process-based models are applied to long-term simulation. The decadal tidal inlet change (Cayocca 2001; Dissanayake and Roelvink 2007), decadal micro-tidal spit-barrier development (Jimenez and Arcilla 2004), millennial tidal basin evolution (Dastgheib et al. 2008) and millennial delta evolution (Wu et al. 2006) were simulated by such models in which promising results were obtained.

Among different types of coastal environment, the barrier islands have the most variable morphology. They

are constantly shaped by winds, tides and waves and, on a longer time scale, they can shift landward or seaward according to the oscillations of sea level and variations in the sediment supply (Masetti et al. 2008). Although the general processes for formation and evolution of barrier islands are well explained by conceptual models (e.g. Schwarzer 1973) and numerical cross-shore models which are based on simplified assumptions (e.g. Masetti et al. 2008), there are very few morphodynamic models that can be used for 2DH area (based on depth-averaged formulations for hydrodynamics and sediment transport) simulation of long-term (decadal-to-centennial scale) morphological evolution of wave-dominated barrier islands. The construction of a long-term 2DH area morphodynamic model for wave-dominated barrier islands is a challenging work for coastal engineers as it not only requires resolving all the different processes acting on different scales related to the morphological evolution but also has to incorporate the influence of climate change. For the former problem, a multi-scale concept has to be integrated in the development of the model for coupling the different modules which calculate the processes at their corresponding temporal and spatial scales. The latter problem needs to be solved at an interdisciplinary basis where knowledge of climate change, sedimentology, geology, oceanography and computer science is combined together. Based on the outcomes of a scientific project named SINCOS (Sinking Coast: Geosphere, Ecosphere and Anthroposphere of the Holocene Southern Baltic Sea, Harff et al. 2007), the authors have developed a modelling methodology for the simulation of decadal-to-centennial (long-term hereafter) morphological evolution of wave-dominated coastal environments and applied it to the Darss–Zingst peninsula at the southern Baltic Sea (Fig. 1). The methodology consists of two main components: (1) a preliminary analysis of the key processes driving the morphological evolution of the study area based on statistical analysis of meteorological data and sensitivity studies; (2) a multi-scale process-based model in which the ‘reduction’ concepts and techniques for morphological update acceleration are implemented.

This paper is organized as follows: in Section 2 we will introduce the geomorphologic features of the Darss–Zingst peninsula. Section 3 describes the ingredients of the model and the multi-scale long-term modeling strategy. The fourth section introduces the generation of representative climate conditions which serve for the model input. Based on the validated model in which coastline change of the research area for the last 300 years was successfully hindcasted, influences of the different scale processes (long-term wave dynamics and short-term storms) on the long-term coastline change of the research area and projected coastline change in the next 100 years are described in Section 5. A summarising discussion is given in Section 6.

Fig. 1 General location of the Darss–Zingst peninsula and coupled grid systems used in the model



2 The study area

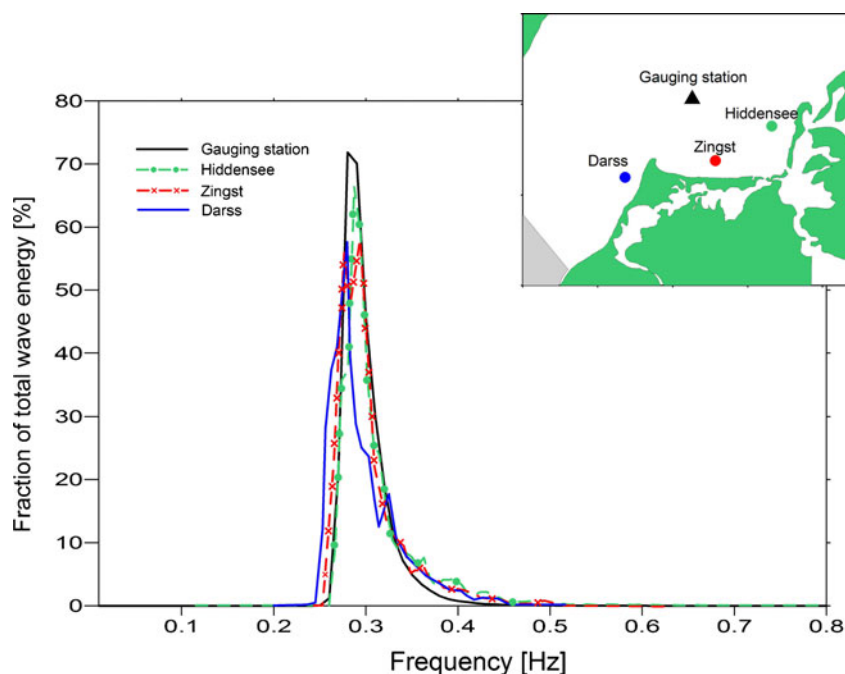
In contrast to other waters, the Baltic Sea distinguishes itself by its high variety of coastal types. In general, moraine material predominates at the southern and south-eastern coasts, while hard bottom and rocky shores are typical in the northern coasts (Schiewer 2008). Hydrodynamics of the Baltic Sea are mainly characterized by complicated meso-to-large-scale wind-driven littoral drifts and local-scale wind-induced waves. Tides coming from the North Sea attenuate quickly after entering the Baltic Sea through a series of narrow channels. Tide range in the southern Baltic area is within 15 cm, while large-scale meteorological situations can excite a surging motion with water level changes in the order of 1.5 m within 1 day; thus, the Baltic Sea can be described as a tideless sea and may serve as an excellent example for studying the coastal evolution under the effects of wave dynamics.

Following the Litorina transgression onset (approximately 8,000 cal BP), the sea level in the southern Baltic Sea has reached a relatively stable level with minor fluctuations in the range of several meters in the last 6,000 years (Kliewe 1995; Schumacher and Bayerl 1999; Muller 2001). The rate of sea-level change is generally between -1 mm/year and 1 mm/year in the southern Baltic Sea in the last 4,000 years (Lampe 2005), which is the same magnitude as neotectonic movements in this area (Harff et al. 2007). Along with the stable sea level and neotectonic conditions, other processes such as climate change, hydrodynamics and sediment transport have become increasingly important for the

coastline evolution (Schwarzer and Diesing 2003). The terrain of the Baltic Sea (Fig. 1) provides a natural sheltering effect in its southern and western part for the wind-induced wave dynamics. The waves induced by the dominant westerly winds in the western and southern Baltic Sea are usually restricted to small amplitudes due to the limited fetch; thus making the southern Baltic coasts more vulnerable to the swells and strong waves induced by the easterly winds which are able to cause a high water level. Figure 2 shows a 10-year (1990–1999) wave spectrum in the offshore area of the Darss–Zingst peninsula. The wave spectrum is a hindcast of a regional wave model which is validated by observational data in several gauging stations (Weisse et al. 2009). It shows that more than 98% of the waves in this area are short waves with a period between 2.5 and 4 s. Such a stable and mild hydrodynamic environment allows a relatively smooth coastal evolution of the Darss–Zingst area in the recent hundreds of years.

The Darss–Zingst peninsula is composed of two main parts. The exterior part is a triangular shaped barrier island with two stretched wings at the south-west (Fischland–Darss) and the east (Darss–Zingst), and a spit (Darsser Ort) linking the two wings at the north. The formation of the barrier island is a result of the combination of climate change, hydrodynamics and sediment transport, which still remains active today. The interior part is a chain of lagoons (so-called Darss–Zingst Bodden) which are subject to a progressive phytogenic silting-up. The westerly exposed coast of the Darss and the northerly exposed coast of the Zingst are characterized by strong abrasion of the cliff coast

Fig. 2 Distribution of wave energy at the corresponding frequencies of four different points in the Darss–Zingst area. Data of three points (Darss, Zingst and Hiddensee) are modeled using the representative yearly wind series; data of the gauging station is a hindcast for a 10-year span (1990–1999) provided by GKSS-Research Centre, Geesthacht



and the flat beach coast, as well as a fast accumulation at the top of the spit (Darsser Ort) due to abundant sediment supply brought by the wind-induced longshore currents. The eastern sequel of the peninsula is the sand flat “Bock” which is separated from the southernmost tip of Hiddensee Island by a dredged channel. The Bock Island is like a container where sediment transported southward along the island of Hiddensee and eastward along the Zingst coast accumulates. The particular evolution of the Darss–Zingst peninsula may serve as a good example to study the coastal evolution under long-term climate change, and has instigated several descriptive and conceptual studies in the last 100 years (Otto 1913; Kolp 1978; Lampe 2002; Schumacher 2002; Meyer et al. 2008).

3 Model setup and long-term modelling strategy

3.1 Model description

Simulation of the decadal-to-centennial morphological evolution of the Darss–Zingst peninsula is based on a multi-scale process-based model consisting of eight main modules to calculate different physical processes that drive the evolution of the specific coastal environment (Fig. 3). The model consists of:

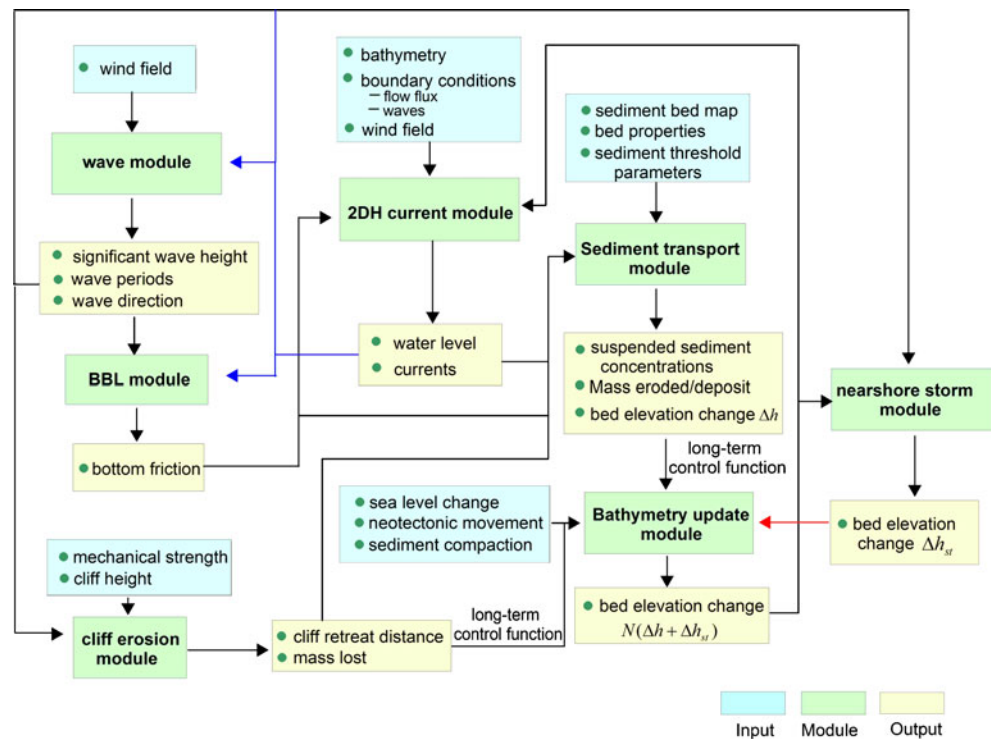
- (1) a 2DH (two-dimensional vertically integrated) circulation module,
- (2) a wind-induced wave module calculating wave parameters for nearshore currents and bottom shear stress,
- (3) a bottom boundary layer (BBL) module calculating the bottom shear stress generated by the combined effects of currents and waves,
- (4) a sediment transport module calculating sediment fluxes,
- (5) a cliff erosion module calculating the lateral sediment fluxes from the cliff and the beach elements,
- (6) a nearshore storm module calculating the sand-dune erosion, overwash and breaching under extreme wind conditions,
- (7) a bathymetry update module calculating the long-term bathymetric change, and
- (8) a long-term control function set up-scaling the processes from short-term to long-term.

The eight modules are designed to couple with one another, with output from one serving as input for another. We mainly introduce the main features of the modules in this paper. Details of the modules are given in Zhang et al. (2010a).

3.1.1 The 2DH circulation module

The Darss–Zingst is a shallow coastal environment with water depth less than 20 m in most of the area. The circulation module is based on the Pearl River Delta-Long-Term Morphodynamic Model, PRD-LTMM (Wu et al. 2007). We have modified the circulation module to include physical processes that are important in the nearshore environment by adding two radiation stress terms (F_x and

Fig. 3 Details of the model coupling framework



F_y) to the vertically integrated shallow water equations, in which currents are computed by:

$$\begin{aligned} \frac{\partial \eta}{\partial t} + \frac{\partial(UD)}{\partial x} + \frac{\partial(VD)}{\partial y} &= 0 \\ \frac{\partial U}{\partial t} + U \frac{\partial U}{\partial x} + V \frac{\partial U}{\partial y} - fV &= -g \frac{\partial \eta}{\partial x} \\ + g \frac{(\tau_{ox} - \tau_{bx})}{\rho D} + \frac{F_x}{D} + v \left(\frac{\partial^2 U}{\partial x^2} + \frac{\partial^2 U}{\partial y^2} \right) & \quad (3.1.1) \\ \frac{\partial V}{\partial t} + U \frac{\partial V}{\partial x} + V \frac{\partial V}{\partial y} + fU &= -g \frac{\partial \eta}{\partial y} \\ + g \frac{(\tau_{oy} - \tau_{by})}{\rho D} + \frac{F_y}{D} + v \left(\frac{\partial^2 V}{\partial x^2} + \frac{\partial^2 V}{\partial y^2} \right) \end{aligned}$$

Where η is the free water surface, U , V are the flow velocity along x and y direction, respectively. D is the water depth defined as $D = H + \eta$ where H is the static water depth. ρ is the average water density, g is gravitational acceleration, f is Coriolis coefficient. τ_{ox} , τ_{oy} represent the surface wind stress which are calculated by the wind-induced wave module; τ_{bx} , τ_{by} represent the bottom stress calculated by the bottom boundary module; v is the eddy viscosity coefficient. F_x and F_y are the gradient terms of radiation stresses resulting from wave breaking. The calculation of radiation stresses was first introduced by Longuet-Higgins and Stewart (1964). In a depth-averaged model, the radiation stresses can be regarded as surface stresses, gradient terms of which are given by

$$\begin{aligned} F_x &= -\frac{1}{\rho} \left(\frac{\partial S_{xx}}{\partial x} + \frac{\partial S_{xy}}{\partial y} \right) \\ F_y &= -\frac{1}{\rho} \left(\frac{\partial S_{xy}}{\partial y} + \frac{\partial S_{yy}}{\partial x} \right) \end{aligned} \quad (3.1.2)$$

where S_{xx} , S_{xy} , S_{yx} , S_{yy} are radiation stresses calculated through the formulation proposed by Longuet-Higgins et al. (1964). An upwind scheme is used in the model to calculate the gradient terms in Eq. 3.1.2.

The current velocities are vertically integrated; hence density current is not taken into account. A robust wet-dry algorithm based on the study of Oey (2005) is embedded in the circulation module to include the simulation of the area which is only reachable by high surges under strong wind conditions.

3.1.2 The wave module

Computation of the wave dynamics is based on a parametric wave model developed in an orthogonal curvilinear coordinate system. The model was first developed by Donelan (1977) and modified by Schwab et al. (1984). It is based on the wave momentum balance equation and employs the JONSWAP spectrum (Hasselmann et al. 1973) to the deep water waves and the TMA (Bouws et al. 1985) spectrum to include the frictional effect on the wave as it moves into shallower water. The wave momentum results from the drag on the waves, which depends on the wave height and the different speeds between the wave and the wind. Given a digital elevation model and a two-dimensional, time-dependent wind field the module calculates significant wave heights, wave periods and wave directions.

3.1.3 The BBL module

Wind-induced waves can significantly influence the bed shear stresses. Bed shear stresses caused by the combined effects of currents and waves can be two orders of magnitude higher than stresses caused by currents alone and may result in significant bed erosion and sediment transport (van Rijn et al. 1993). Generally, the oscillating flow generated by wind-induced waves will reach down to the sea bottom if the water depth is shallower than half of the wave length. In the Darss–Zingst area with strong waves of 5 s under storm conditions, the maximum penetration can be deeper than 19 m, which covers a large fraction of the coastal area; therefore, the effect of wind-induced waves on the sea bed is a critical factor influencing the Darss–Zingst coastal environment.

A modified version of the Grant-Madsen model (Grant and Madsen 1979) with movable bed effects on the physical bottom roughness which was developed by Glenn and Grant (1987) is incorporated in the BBL module. The parameter setting of the BBL module is mainly based on the study of Kuhrt et al. (2004), in which the application of the BBL module to the Baltic Sea was carried out.

3.1.4 The sediment transport module

The sediment transport module is based on the PRD-LTMM model and improved from the framework of ECOMSED (Estuarine Coastal Ocean Model with SEDiment) (HydroQual, Inc. 2002). It consists of three parts: (1) simulation of cohesive sediment (silt/clay) transport; (2) simulation of non-cohesive sediment (fine and medium sand) transport, and (3) simulation of coarse sand transport. Transport of the first two types of sediment is dominant in the coastal environment as they are taking up a majority of the bed material. The transport of coarse sands (transported as bed-load in the model) is important in the nearshore area (with water depth from 0 to 10 m) of the southern Baltic Sea for the migration of sand bodies (Schwarzer and Diesing 2003). The bed-load transport of coarse sand is calculated by the Bailard equation (Bailard 1981).

The cohesive and non-cohesive sediment are transported as suspended particles. The two-dimensional horizontal equation for both types of sediment is given by:

$$\frac{\partial DC}{\partial t} + \frac{\partial DuC}{\partial x} + \frac{\partial DvC}{\partial y} + De - Er - \varphi_{\text{source}} = \frac{\partial}{\partial x} \left(DA_h \frac{\partial C}{\partial x} \right) + \frac{\partial}{\partial y} \left(DA_h \frac{\partial C}{\partial y} \right) \quad (3.1.3)$$

where C is the suspended sediment concentration; De represents deposition flux and Er represents resuspension flux. Calculation of these two parameters is following the framework of ECOMSED (HydroQual, Inc. 2002). The horizontal eddy diffusivity (A_h) is calculated using the Smagorinsky eddy parameterization (Smagorinsky 1963).

The term φ_{source} denotes the sediment source term from the lateral boundary (by erosion of the cliff and sandy beach):

$$\varphi_{\text{source}} = \begin{cases} 0, & \text{for non-lateral boundary cells} \\ \varphi_{\text{lateral}}, & \text{for lateral boundary cells} \end{cases}$$

3.1.5 The cliff erosion module

The coast of the southern Baltic Sea is composed of cliffs and sandy beaches. According to the study of Diesing et al. (1999), the material from the erosion of cliffs in the southern Baltic (Pomeranian Bight) is at the order of 10^6 t/year. An average retreat of coastline amounts to 50 cm/year at Darss and 100 cm/year at Zingst (Fig. 4), which indicates the cliff erosion (here includes beach erosion) as an important factor influencing the long-term morphological evolution of the southern Baltic Sea.

Coast erosion is complicated, it is caused by a variety of natural behaviours such as sea-level rise, variation in sediment supply, waves, storm surges, ice cover, long-shore sediment removal and transport, and sorting of sediment on the beach under wave actions. Anthropogenic activities make it even more difficult to predict the coast recession at a long-term scale. In the model we neglect effects of other processes and consider only two basic factors controlling cliff erosion in the research area: (1) the force of waves at the base of cliffs, and (2) the mechanical strength of the cliff component (e.g. hard-rocks, glacial tills and sands). A parametric relation between the wave force and coastline erosion is developed based on the study of Sunamura (1992).

The erosion rate is expressed as

$$R' = \begin{cases} \frac{K}{T'} \ln \left(\frac{F_w}{F_r} \right), & F_w > F_r \\ 0, & F_w \leq F_r \end{cases} \quad (3.1.4)$$

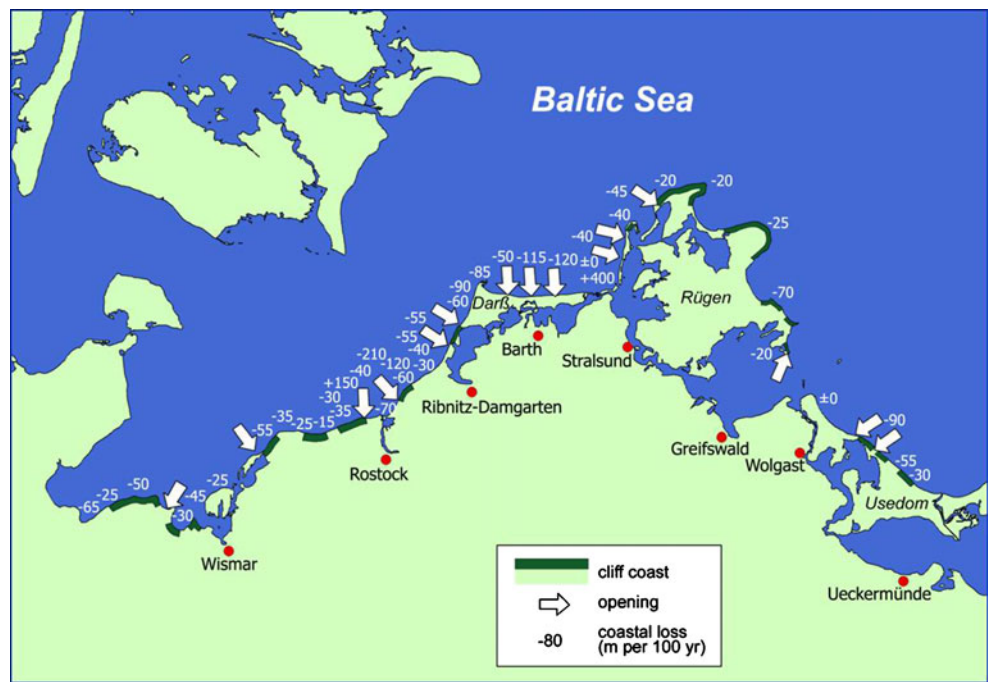
where R' is the erosion rate within one wave-period (m/s); $T' = \frac{365 \times 24 \times 3,600}{T_{\text{wave}}}$ where T_{wave} represents the instant wave period. K is a constant with the physical dimensions of a velocity; F_r is the mechanical strength of the cliff (MPa); F_w is the destructive force of the waves (MPa) which is given by

$$F_w = \sin \theta \left(\frac{\rho g H^2}{8} \right) C_n \quad (3.1.5)$$

where θ is the angle between the direction of wave propagation and the wall of the cliff. H is the significant wave height at the base of the cliff; C_n is the group velocity of the waves. Values of these parameters are provided by the wave module.

Considering that the Darss–Zingst peninsula is mainly composed of clastic sediment, the components of the cliffs are assumed as sands with silt and clay, which has a relatively low

Fig. 4 Measured coastline change in the southern Baltic during the twentieth century (after Staun Rostock 1994). Negative number denotes coast-line retreat distance



compressive strength and incompact adherence. $F_r=0.1$ for glacial till cliffs is set in the module according to (Budetta et al. 2000). Since the bathymetry is treated in a discretized form in grid cells in the model (Fig. 5), the whole coastline (the sandy beaches are treated as ‘dune cliffs’) is included in the calculation of ‘cliff’ erosion. Sensitivity studies indicate that $F_r=0.02$ is suitable for ‘dune cliff’ elements in the module to produce a coastline change similar to the measured data (Zhang et al. 2010a).

The eroded material from the cliff serves as the source term for the sediment transport equation Eq. 3.1.3, which is given by

$$\varphi_{\text{source}} = \begin{cases} f_{\text{coh}} \frac{R' \Delta x H_{\text{cliff}}}{T_{\text{wave}}}, & \text{for silt/clay;} \\ (1 - f_{\text{coh}}) \frac{R' \Delta x H_{\text{cliff}}}{T_{\text{wave}}}, & \text{for sand.} \end{cases} \quad (3.1.6)$$

where Δx is the grid cell width at the cliff; H_{cliff} is the cliff height; f_{coh} is the fraction of cohesive sediment of the eroded material. $f_{\text{coh}}=0.7$ is assumed for the glacial till cliff elements according to the study of Emeis et al. (2002) and 0.1 for ‘dune cliff’ elements.

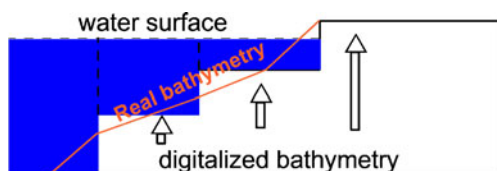


Fig. 5 The whole coastline is included in the calculation of ‘cliff’ erosion in the model (Zhang et al. 2010a, Zhang et al. under review)

One shortcoming of the module is the error induced by the orthogonal curvilinear grid system used in the calculation of cliff erosion. The orthogonal grid cannot correctly fit the irregular coastline (Fig. 6), thus Cells 1 and 2 are digitalized as land cells where cliff erosion is calculated. The coastline erosion at these cells may be overestimated in the model because the model calculates erosion of two sides (e.g. side $X1$ and $X2$ of Cell 1) rather than one side at these cells. The calculated instant erosion is not overestimated if the wave is coming perpendicular to the side $X2$ (e.g. Wave 1 shown in Fig. 6) as the wave force is zero at side $X1$ according to Eq. 3.1.5. However, errors are generated when the wave is coming from a direction as Wave 2. Assuming the length of $X1$ equal to the length of $X2$ and the angle between the wave direction and the wall of both sides are the same (45°), the calculated instant erosion will be twice as the real erosion in such a case. One way used in the model to handle this problem is marking the cliff elements similar to Cells 1 and 2 and smooth the overestimated

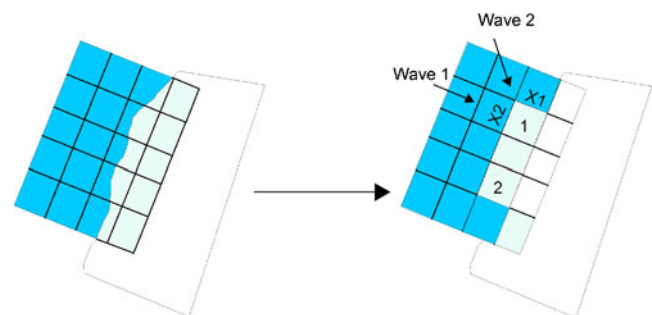


Fig. 6 Digitalization of the coastline in an orthogonal grid system

erosion by averaging the erosion at these cells with their neighbour cells which only have one side.

3.1.6 The nearshore storm module

The nearshore storm module aims at calculating the short-term coastline change caused by storms. It runs separately from other modules and is activated according to the frequency of a north-easterly storm happened in the Zingst coast which is vulnerable to such storms indicated by sensitivity studies (which will be described in section 4). The nearshore storm module is based on the XBeach model developed by Roelvink et al. (2009). XBeach is a 2DH model that allows a high-resolution domain to solve coupled equations for short-wave energy, flow, infragravity wave propagation, sediment transport and bed-level change on the time scale of wave groups. It is able to simulate the small-scale processes related to storm impacts on the coastline area such as depth-averaged return flow, long-shore currents, swash, overwash, backwash, dune slumping and suspended sediment transport. The model has been extensively validated in 1D flume experiments and 2D field cases (Roelvink et al. 2009; McCall et al. 2010). A detailed description of the XBeach model is given by Roelvink et al. (2009). The XBeach model does not calculate the wave conditions and water levels at the offshore open boundary. These parameters are provided by the local model.

3.1.7 The bathymetry update module

The bathymetry update module is a part of the long-term modelling methodology. Bathymetrical update in our model is divided into two parts. One part is real-time update which updates the bathymetry after every time step of sediment transport calculation (which will be further explained in Sec 3.2.5) and the other part is long-term update. The long-term bathymetrical update is based on the concept that the sea bottom evolves much slower than the flow pattern, and assuming that the flows and waves are not affected by small changes in the bathymetry until the calculated bed changes exceeds a pre-defined value ε which may significantly influence the flow field. A parameterization of $\varepsilon = \text{Min}(0.4 \text{ m}, 0.2H)$ is set in the module (which will be explained in Section 3.2.5), where H is the water depth of the local grid element. Once the pre-defined value is reached, the bathymetry update is given by

$$\Delta H_{n+1} = mf \times \left(\sum_{k=1}^M \Delta \lambda_k \Delta z_k - \Delta D_{n+1} + \Delta E_{n+1} + \Delta SL_{n+1} - \Delta \gamma_{n+1} + f_s \Delta z^s \right) \quad (3.1.7)$$

where ΔH_{n+1} is the bed elevation change (unit: m) during the $(n+1)$ th cycle of hydrodynamic computation; mf is a

morphological update factor (which will be further explained in Sec. 3.2.5); Δz_k is the thickness (unit: m) of the k th layer of the condensable sediment ($1 \leq k \leq M$, where M is the user-defined number of condensable sediment layers above the marine base); ΔD_{n+1} and ΔE_{n+1} are the thickness (unit: m) of sediment deposition and erosion in the $(n+1)$ th cycle of model run calculated from the representative yearly wind series, respectively. ΔSL_{n+1} is the sea-level change (unit, m) for the $(n+1)$ th cycle of computation (a rise is positive); $\Delta \gamma_{n+1}$ represents the corresponding neotectonic movement (an uplift is positive, unit: m). f_s is the frequency of a representative north-easterly storm (which will be further explained in Section 4) and Δz^s is the calculated storm-induced bathymetrical change. λ_k is the long-term compaction rate (%) for the k th layer of the condensable sediment, which is given by Wu et al. (2007).

3.1.8 The long-term control function set

The long-term control function set is a composite of functions that relate to long-term computation in the model. It includes (1) functions for extending the processes from short-term scale to long-term scale, and (2) functions for error analysis and auto-regulating the input parameters by calibration during the continuous model computation cycles.

Functions of the first type are embedded in different modules to combine the multi-scale processes, e.g. the calculation of long-term bathymetrical change and coastline change by multiplying the morphological update factor to the real-time calculation values after each cycle of model computation. Functions of the second type mainly serve for calibration of the model, e.g. to regulate the trend of river discharge, boundary sediment input, representative wind input series and sea level variation for different time periods which are based on statistical analysis and to stop the model run and indicate the errors if a biased result is produced by comparison of the calculation results to reference data which is available.

3.2 Long-term modelling strategy

The processes influencing the coastal morphological evolution generally happen at different temporal and spatial scales. Direct numerical simulation of all different-scale processes on a single grid system poses formidable computation challenge (large memory and computation time requirements) as the grid resolution and the calculation time step are determined by the smallest-scale process. In order to solve this problem, multi-scale concepts are integrated in our model development. Multi-scale modeling aims at providing a solution of computation of different-scale processes. It allows resolving the processes at their

corresponding scales and extrapolating the effects of short-term processes to a long-term period without causing any calculation instability. Integration of multi-scale concepts in our modeling work is realized as follows.

3.2.1 Evaluation of different-scale wave processes

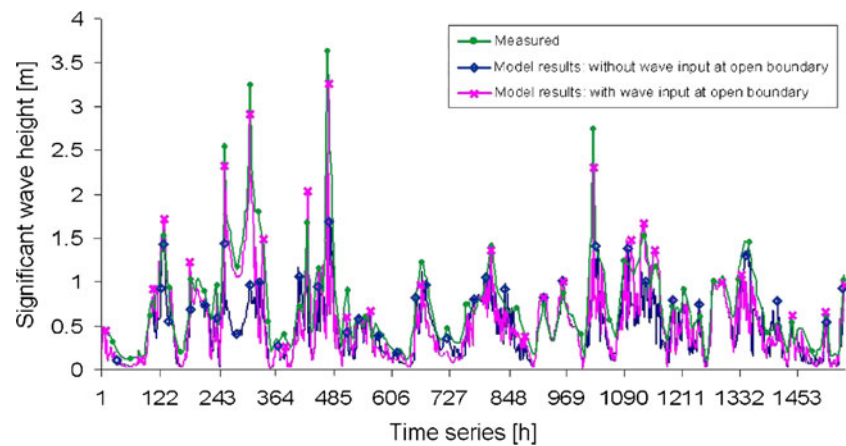
Decadal-to-centennial-scale simulation cannot take into account the most refined representation of all physical processes, thus each module is run under certain approximations regarding processes and input parameterization. As the tidal effects are neglected in the model, the wind-induced waves play the dominant role in the hydrodynamics. The purpose of our model is to resolve the main driving terms of the long-term morphological evolution of the research area. Wave processes are separately evaluated in our modelling strategy. In the nearshore storm module which simulates the storm-induced erosion of the Zingst coastline area, small-scale processes related to wave breaking and overwash are calculated; In the local model (which will be described in Section 3.2.2) which is used to simulate the long-term morphological evolution, only the following wave properties are modelled: (1) the enhanced bottom shear stress caused by combination effects of currents and waves; (2) the radiation stresses at the water surface due to the wave breaking; (3) wave energy at the lateral boundary. As the processes are modelled in a two-dimensional vertically integrated scheme, vertical processes such as undertow and wave asymmetry are not included. Neglecting the small-scale vertical processes (undertow and wave asymmetry) might lead to underestimation of the cross-shore sediment transport in the model. However, the hindcast results are still in good agreement with the measured data, which indicates that the longshore sediment transport and the cross-shore sediment transport induced by longshore variation of the radiation stresses and bathymetry play a dominant role in the long-term morphological evolution of the Darss–Zingst peninsula. A more detailed discussion of the cross-shore sediment transport will be given in Section 6.

3.2.2 Grid coupling

The Baltic Sea itself forms a complete coastal system. Any local part of it is under the influence of larger-scale regional hydrodynamic movements such as wind-driven circulations and water level variation induced by extreme wind events. Thus, any modelling of a local coastal area must include the influences of regional-scale hydrodynamics; otherwise large biased results may be generated. On the other hand, the morphodynamic modelling of wave-dominated systems requires solving the processes related to sediment transport in detail, in which a high-resolution computation grid is

needed (especially within the surf zone area where wave breaking happens). Simulation of processes in a high-resolution grid which covers a large area is an extremely time-consuming work even by today's computer power, especially for long-term modelling. In order to solve the problem of computation time and to capture all the different-scale processes which are important for coastline evolution, grid coupling is introduced. Three different grids (as shown in Fig. 1) are designed in our modelling work to calculate the processes at their corresponding scales, and results of the larger grid serves as boundary inputs for the smaller grid. The regional grid which covers the whole Baltic Sea is used to calculate the wind-driven circulations and waves under a large wind fetch. As these processes generally happen on a large scale, a grid resolution of 1 nautical mile (1,852 m) is capable to resolve these processes in the southern Baltic Sea (Seifert et al. 2009). In our modelling work, a resolution of 1,000 m in the southern and south-western Baltic Sea and 10,000 m in the northern Baltic Sea is used for the regional grid. As the regional grid is not related to the sediment transport calculation, only the circulation module and wave module are activated in the calculation. The output wave parameters and flows serve as open boundary conditions for the local model. For the decadal-to-centennial modelling, we assume that the large-scale flows and wave patterns are not influenced by the coastline change of local areas, thus the regional model is only executed once. The open boundary conditions for the local model remain the same during the continuous cycles of runs (where long-term calculation is implemented). The open boundary conditions (waves, flows) are very important for the local hydrodynamics as they provide necessary additional momentum for the growth of local waves and flows. Figure 7 shows the differences between the calculated significant wave heights by the local model with and without open boundary inputs at a gauging station which is located in the offshore area of Darss–Zingst. The main disadvantage of the calculation without open boundary inputs is the underestimation of wave heights under strong wind conditions. Two continuous eastern storms (294 and 480 h) and one strong westerly wind event (1,015 h) happened in the 2-month period. The calculation without open boundary inputs is able to generate similar significant wave heights to the measured data during the western storm as wave growth driven by westerly winds in the Darss–Zingst area is restricted by the terrain of the south-western Baltic Sea. What should be noted is the wave growth under the strong easterly wind conditions (294 and 480 h). The bias between the calculation without open boundary inputs and the measured data is remarkable (i.e. the increase of wave heights is not reflected without open boundary inputs). The gap between the calculated wave heights and measured data is filled by inclusion of open boundary inputs, which indicates the necessity of coupling of the regional grid

Fig. 7 Comparison between the calculated significant wave heights in the local model with and without wave boundary input from the regional model. Simulation time starts at 01:00 Jan 1, 2000



with the local grid for better reflecting wave dynamics under strong wind conditions.

A local grid which covers the whole Darss–Zingst area is designed to calculate the processes related to long-term morphological evolution. Such processes include bottom boundary layer under the combined influence of currents and waves, wave breaking, longshore currents, shoreline erosion and littoral sediment transport. As these processes generally happen on a small scale from several meters to several hundred meters, high resolution in the cell size is needed to accurately calculate these processes. However, higher-resolution grid also requires more CPU time (CPU time is the amount of time for which a Central Processing Unit was used for processing instructions of a computer program); this could make the CPU time for long-term modelling become unacceptable, especially for centennial-scale modelling. Thus, the design of the grid resolution to make both the accuracy of calculation and CPU time acceptable is an important step in the long-term modelling work. Several experimental runs were carried out to study the effects of grid resolution, which will be described in Section 3.2.3.

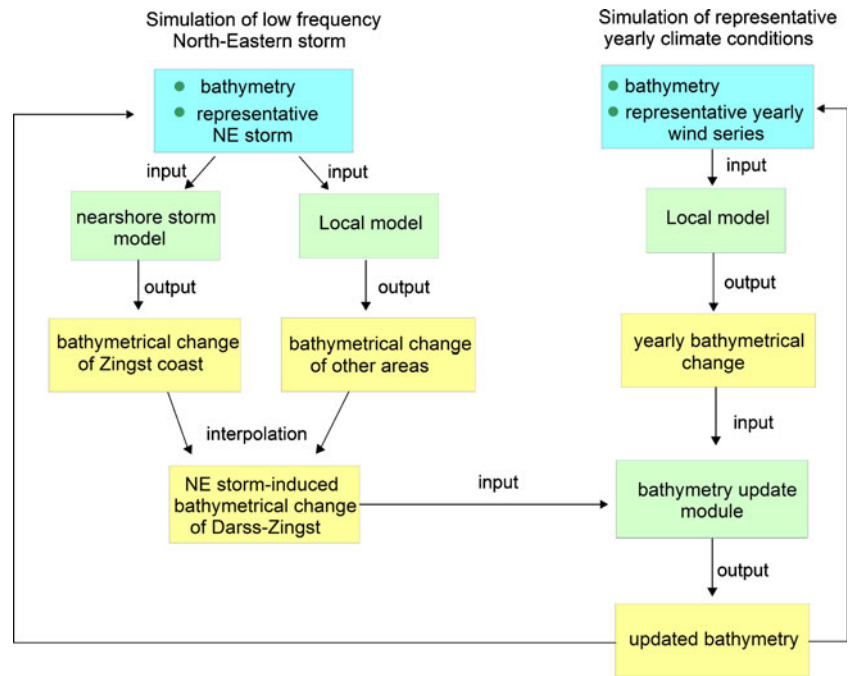
The local grid reads open boundary conditions from the regional grid and outputs open boundary conditions for the nearshore grid, which only covers the lowland part (with elevation <5 m above the mean sea level) of the Zingst coast and its surf zone. In the inundated sandy areas during storms, processes such as dune erosion, overwash, breaching and sediment slumping from dune erosion dominate. In order to simulate these processes, the nearshore storm module has to be run on a high-resolution grid. Therefore, a rectilinear nearshore grid with high resolution of 5 m in the cross-shore direction and 50 m in the long-shore direction of the Zingst coast is designed for the nearshore storm module. As the frequency of a north-easterly storm is once every 5 years (according to results of the statistical analysis of the wind data and sensitivity studies described in Section 4), it allows the decoupling of the nearshore storm module with other modules to save the computation time. Open boundary

conditions for the nearshore grid which are provided by the local model are fixed in every run of the nearshore storm module based on the assumption that the offshore wave parameters and currents do not change in a representative storm at the decadal-to-centennial scale. What runs in ‘parallel’ between the two grids is the update of the bathymetry. The nearshore storm module reads the updated bathymetry from the local model and calculates the storm-induced bathymetrical change. The calculated bathymetrical change in the nearshore storm module is then interpolated and added to the local grid system in which the North-East (NE) storm-induced change in other areas are calculated. The resultant storm-induced bathymetrical change of the whole Darss–Zingst peninsula is stored to the path where the bathymetry update module reads after one cycle of calculation on the local grid using the representative yearly wind series. The bathymetry module then determines the morphological update factor mf (which will be further explained in Sec 3.2.5) and yields the extrapolated (by multiplying mf) bathymetrical change described in Eq. 3.1.7 and output the updated bathymetry which is both needed by the local model and the nearshore storm module for the next cycle of calculation. The procedure for one cycle of calculation is explained in Fig. 8. The nearshore grid is only used to calculate the low-frequency NE storms and designed to run in parallel with the local model, thus no extra CPU time is caused. Such a grid coupling enables the incorporation of all important processes relevant to coastal morphological evolution and calculation of these processes at their corresponding scales.

3.2.3 Grid resolution

Design of grid resolution is a critical step in the long-term modelling work as it not only influences the accuracy of calculation results but also determines the CPU time needed for the whole simulation. The choice of grid resolution in our modelling work follows several considerations: 1. the

Fig. 8 Calculation procedure of the coupled nearshore storm model and local model. Each loop indicates one cycle of calculation



spatial scale of the processes of interest; 2. the error between simulation results and measured data; 3. the CPU time needed for calculation. For the regional grid (with a resolution of 1,000 m in the south-western Baltic Sea) and nearshore grid (with a resolution of 5 m in the cross-shore direction), the processes are calculated at their corresponding spatial scales and satisfying results are obtained within acceptable CPU time. This is because only a limited number of processes are considered in these grids and no long-term calculation is involved. The main challenge of the resolution choice lies in the local grid, in which all important processes related to centennial-scale coastal morphological evolution are calculated in a series of iterative runs. In order to obtain the optimum grid design for the local model, three runs with different grid resolutions are carried out. Run01 has a resolution of 300–400 m in the Darss and Zingst coastline area; Run02 has a resolution of 100–200 m in the coastline area, and a resolution of 50–150 m in the coastline area is designed in Run03. Figure 9 shows the difference between results of Run01 and Run02 in the spit area. As can be seen from the pictures at the top, the circulation pattern at the east side of the spit and the wave breaking effect on the currents along the coastline are not well resolved in Run01. Such difference in grid resolution leads to large divergence between the calculated morphological changes after a long-term run, which are shown in the pictures at the bottom. The growth of the spit is completely stopped by erosion at the spit in Run01, and deposition at the east side of the spit is far from the measured data. By comparing the bathymetrical changes in Run01 and Run02, we can see that most of the sediment is deposited in the

upward offshore area of the spit rather than its east side in Run01. This is due to the relatively rough grid resolution in which the small-scale flow pattern around the spit is not well resolved. By contrast to Run01, with a resolution of 100 m in some sensitive areas (Darsser Ort, Bock) and 150–200 m in other coastline areas, Run02 is able to generate the results that are closer to the measured data (Fig. 9, right panel). As wave breaking generally happens within a narrow surf zone (100–300 m from the coastline) in the Darss–Zingst area, a higher-resolution grid in Run03 is more accurate in resolving wave breaking, however, the CPU time needed for a long-term run (20 years) is doubled in Run03 compared to Run02. This is not only caused by the increased grid resolution but also by the limitation of the Courant–Friedrichs–Levy condition, which only allows a smaller time step in a higher-resolution grid to maintain the stability of model calculation. In order to get clearer ideas about the effects of grid resolutions on the long-term coastline change of the Darss–Zingst peninsula, coastline change of 100 years (1900–2000) are calculated in the three runs and results of 26 points along the coast are shown in Fig. 10. The differences of calculated coastline changes between Run01 and the other two runs are obvious. Coastline erosion along the Darss area is greatly underestimated in Run01 by a root mean square error (RMSE) of 23 m and so does the growth of the spit. The calculated coastline changes along Zingst are similar in all three runs as these values are mainly calculated in the nearshore grid. Differences between the results of Run02 and Run03 are not distinct with a RMSE of 7 m, which

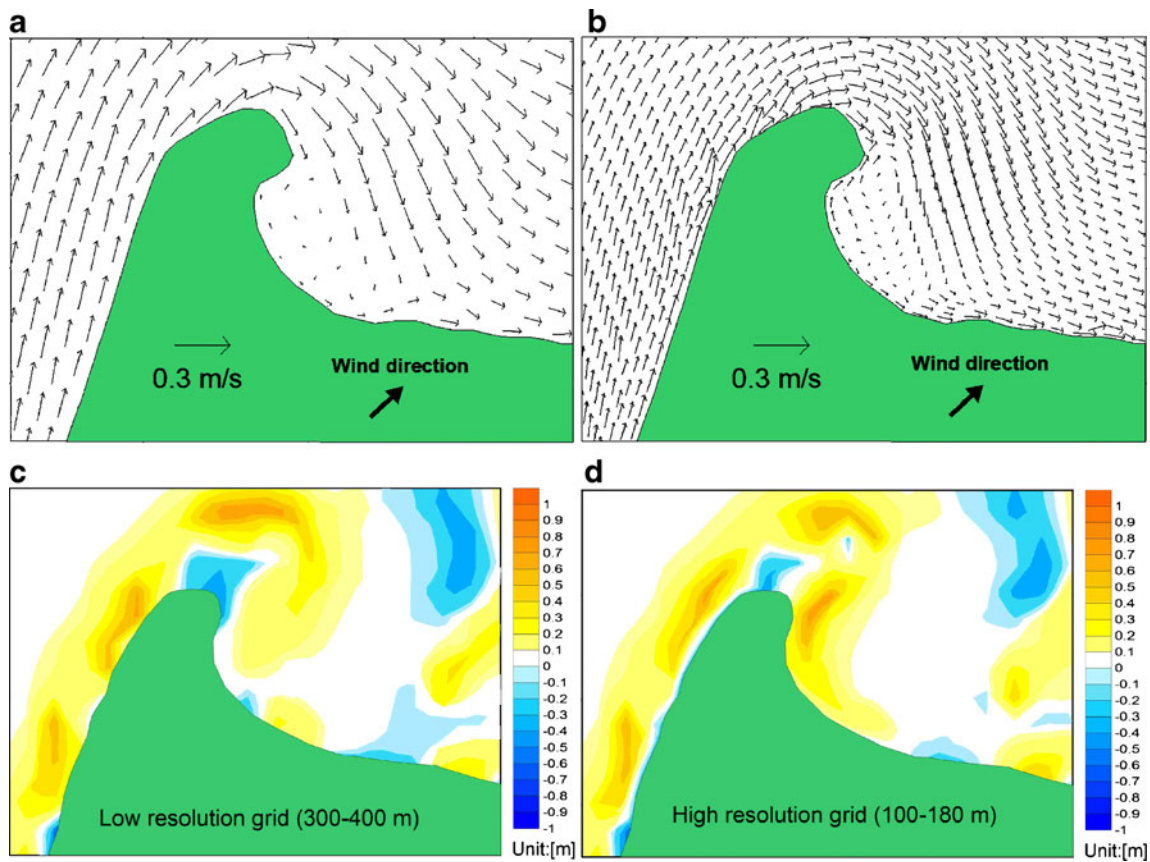


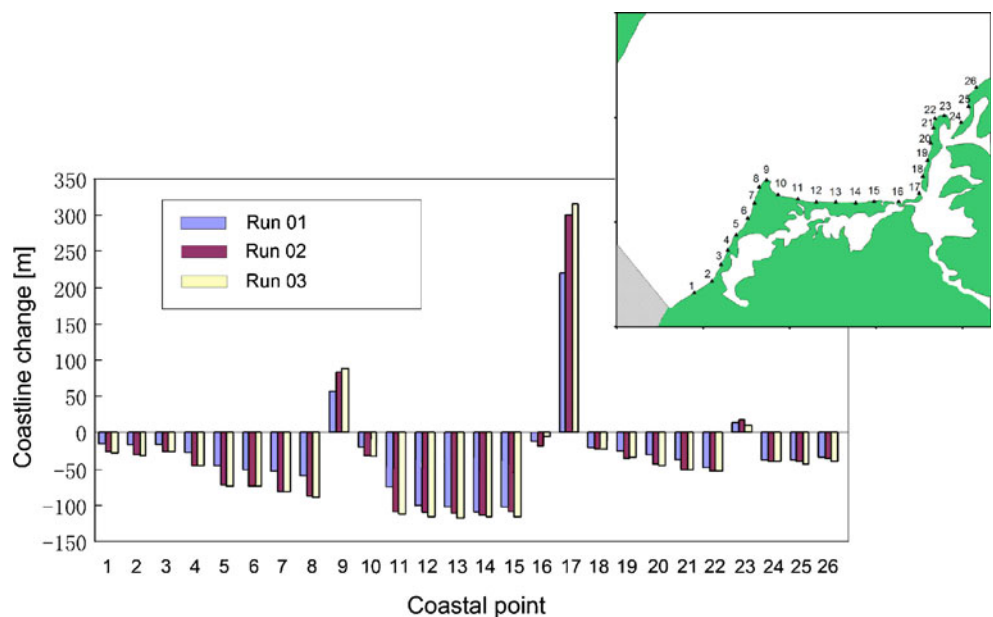
Fig. 9 **a** Flow field with a resolution of 300–400 m in the coastline area; **b** Flow field with a resolution of 100–180 m in the coastline area; **c** and **d** Bathymetrical change after a 20-year simulation with the different resolutions

indicates that a resolution of 100 m in sensitive areas (Darsser Ort, Bock) and 150–200 m in other coastline areas is enough to reflect the effects of the main processes on the long-term morphological evolution of the Darss-Zingst peninsula within acceptable CPU time.

3.2.4 Evaluation of long-term climate change

As the long-term simulation is based on the concept of ‘reduction’ (de Vriend et al. 1993a, b; Latteux 1995) to solve the problems of boundary input due to the lack of

Fig. 10 Simulated coastline changes (1900–2000) with different grid resolutions. Positive number indicates accretion and negative number indicates erosion



detailed time series of data covering such a long time span and computation time, the concept of representative monthly wind series is introduced in our study to serve as input for the model. Results of statistical analysis of 50 years (1958–2007) wind data in the southern Baltic Sea indicate that the winds of a year can be classified into four seasonal wind classes (a detailed description of representative wind series is given in Section 4). Four representative monthly wind series are generated to ‘represent’ these seasonal classes, respectively. A representative monthly wind series is composed of 720 (hours of a month) synthetic wind elements. The representative wind series are generated by statistical analysis of the 50-year high-resolution (hourly) wind data in the southern Baltic Sea and corrected by sensitivity studies in order to obtain the wind spectrum that induces approximate coastline change to the measured data in the last century. It is able to reflect statistically the features (spectrum) of a seasonal wind class and thus represents all the months of one class. The use of representative monthly wind series is related to the long-term modelling strategy of the bathymetric update. The model calculates for only one representative wind series instead of all the months it represents, thus being able to save CPU time. The validity and reliability of the representative wind series is proven by comparison between the measured data and the results of the model in which the coastline change of the Darss–Zingst peninsula for the last 300 years is simulated.

3.2.5 Morphological update

Morphological update of the model domain in our long-term modelling is based on two approaches. The morphological update within the calculation of each representative wind series is similar with the ‘online approach’ (Lesser et al. 2004; Roelvink 2006). In the ‘online approach’ the flow, sediment transport and bathymetrical update are all run at the same small time steps and the calculated bed change after each time step is multiplied by a constant morphological factor n , so that after a simulation of 1 day the model has in fact modelled the morphological change for n days. The difference between the ‘online approach’ and our model is that we are using different time steps for the flow and sediment transport (the hydrodynamic time step is 30 s and the sediment transport is 180 s) and different morphological update factors for different representative wind series. The bathymetrical update within one cycle of model calculation is following the same time step as the sediment transport (180 s). For the calculation of the representative wind series 1, a morphological update factor $n=5$ is used as the wind series 1 represents 5 months (from Oct to Feb). For the calculation of the representative wind series 2 (represents 3 months from Mar to May) and series 3

(from Jun to Aug), a morphological update factor $n=3$ is used. No morphological update factor is used in the calculation of representative wind series 4 (Sep) and the representative annual West-North-West (WNW) storm. With such an approach, the model produces the morphological change for 1 year by calculating 4 representative monthly wind series. The morphological update factor used in our model is small enough to maintain the stability of flow and sediment transport calculation (Roelvink 2006). Another approach called the ‘straightforward extrapolation’ is used after each full cycle of model calculation. After each call to a full cycle of model calculation, the resultant 1 year’s bed-level change is multiplied by another morphological update factor mf which satisfies:

$$\max\{mf \times (\Delta z + f_s \Delta z^s + T)\} \leq \varepsilon \quad (3.2.1)$$

where Δz is the yearly bed-level change calculated by the local model; f_s and Δz^s are defined in Eq. 3.1.7. T denotes the combination effects of other processes (sea-level change, neotectonic movement and sediment compaction) on the yearly morphological change. The determination of the critical value ε is another critical step in the morphological update method. As ε is related to the local water depth H , biased results can be generated on the shallow water cells if ε is too large. Three sensitivity experiments were carried out to determine the maximum value of ε by comparing the calculated coastline change at 26 points along the coast (as indicated in Fig. 10) to the reference results of Run A in which $\varepsilon=H/10$ is set. $\varepsilon=H/5$ is set in Run B and a $\varepsilon=0.3H$ is set for Run C. The time period for simulation is 20 year. The ratio of results of Run B and Run C to the reference results of Run A is shown in Fig. 11. It is shown that a value of $H/5$ for ε is able to produce similar results to the reference result while discrepancy starts to develop when ε increases to $0.3H$. This suggests $\varepsilon=H/5$ is an appropriate critical value for the trigger of bathymetry update. By these two approaches in the model, we get mf year’s bathymetrical change by calculation of four representative wind series. The calculation procedure with the representative wind inputs in the model is described in Fig. 12. The advantage of the morphological update method is that it is able to save CPU time and ensures a smooth evolution of the bathymetry; however, there still remains a problem to be solved. For an area that is becoming increasingly shallow, the efficiency of the morphological update is greatly hindered as ε becomes smaller and a full cycle of model calculation has to be carried out more frequently. One way to solve this shallow water problem is to ‘partly freeze’ these shallow water elements. As the flows and waves on the shallow areas are not able to induce drastic change of the sea bottom elevation under mild weather conditions, a smooth evolution of these cells is assumed. The suspended sediment transport in these shallow

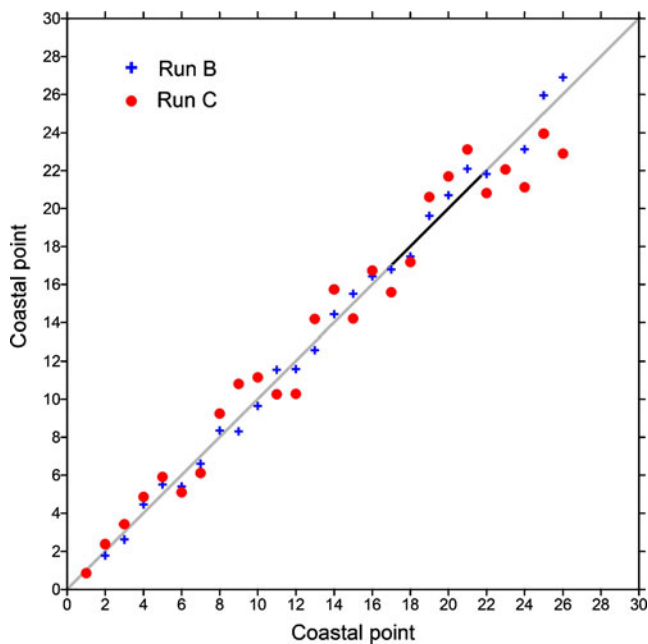


Fig. 11 Ratio of calculated coastline changes at 26 points in Run B and Run C to the reference results of Run A. The solid line indicates identical change to the reference result

cells is not fully calculated in the model to maintain the stability of sediment transport calculation, which means the resuspension flux E_r and deposition flux D_e are fixed to zero in Eq. 3.1.3 during the model run. Only the calculation of the bed-load transport (which is of a very low rate under mild weather conditions) remains normal. Full calculation of suspended sediment transport in these cells will only be enabled when a high stand of water level (during storms) happens to make these shallow water cells become deep water cells. The calculation of ε depends on the deep water

cells rather than the shallow cells in this way, thus allows a larger morphological update factor mf . The shallow water cells are ‘partly frozen’ as only the bed-load transport is calculated and bed-level changes of these cells are not considered in the calculation of mf , but just stored in the model to calculate the final bed-level change after the n th cycle of calculation by multiplying mf . As mf is larger than being calculated by shallow water depth, the final bed change of shallow cells (by multiplying mf) may be large enough to make the water cells become terrestrial cells. If so, these cells will be treated as lateral boundary cells in the cliff erosion module. In order to distinguish the ‘shallow water cells’ from the ‘deep water cells’, a water depth of 1.5 m serves as the critical value in the model. Although it is not completely correct in physics to neglect suspended sediment transport in shallow water cells and to allow a straightforward transition of shallow water cells to terrestrial cells, this method proves to be an efficient way in accelerating the long-term calculation without causing any instability. Hind-cast of the coastline change of the Darss–Zingst peninsula for the last 300 years indicates that the error between simulation results and measured data is within an acceptable range (as shown in Fig. 13).

4 Representative climate conditions

Representative input conditions for the long-term process-based model are based on the concept of ‘input filtering’ (de Vriend et al. 1993a, b), the calculated bathymetrical change based on the representative input conditions should be the same as calculated from the measured input conditions at a long-term period. The time series of winds

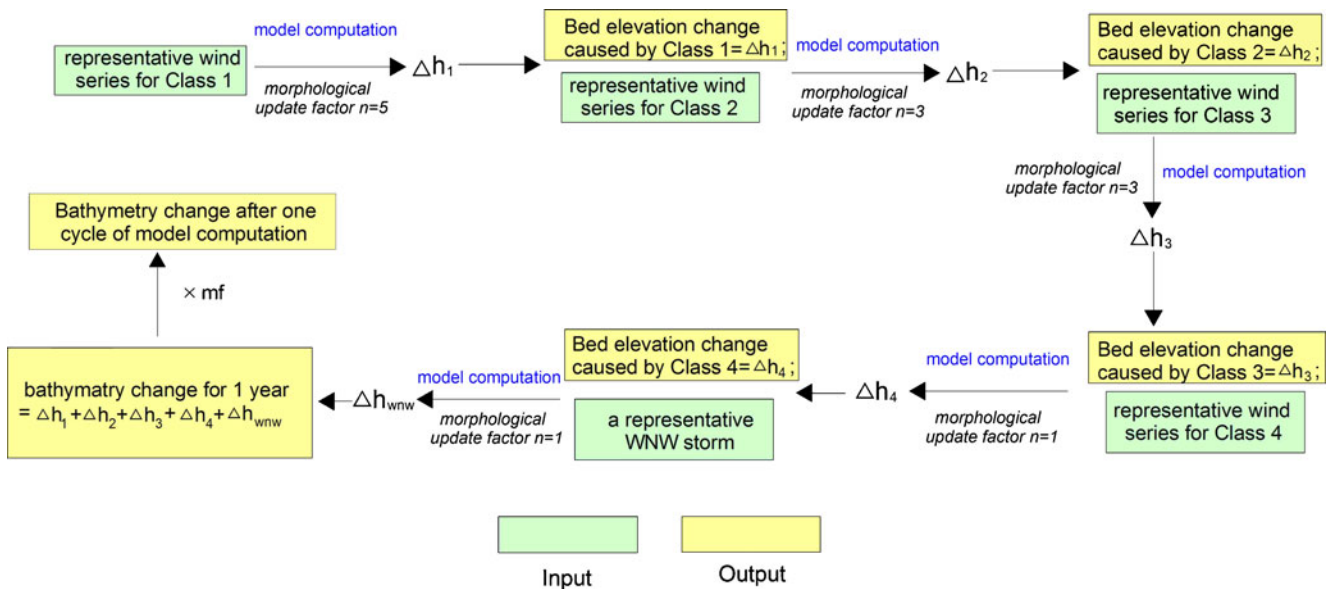
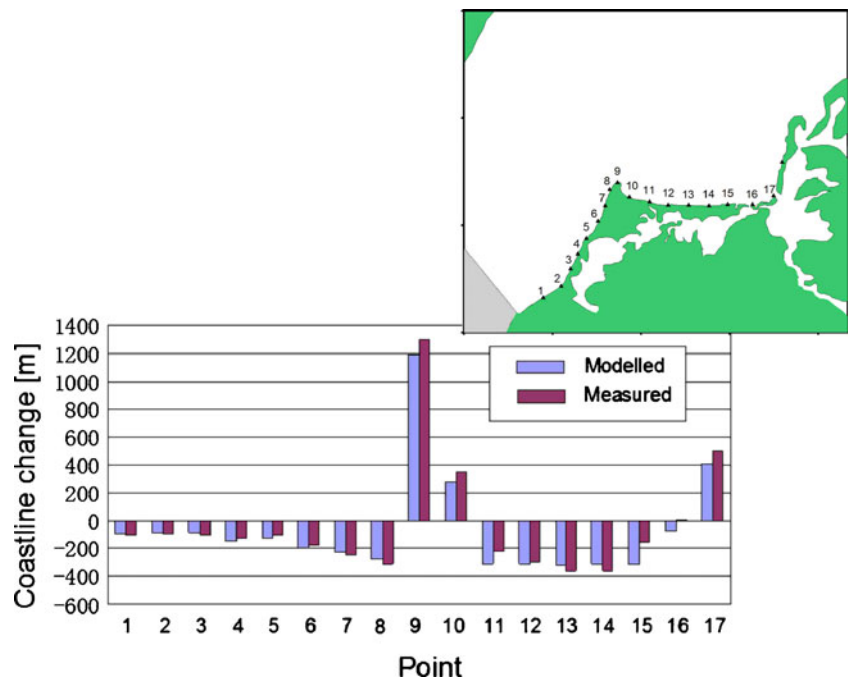


Fig. 12 Calculation procedure of the representative yearly wind series in the model

Fig. 13 Comparison between the modelled coastline and the measured data (Zhang et al. 2010a, Zhang et al. under review)



are needed for the generation of representative input conditions for the model. In this study we use the historical wind series (covering the whole Baltic area with a resolution of 50 km) from 1958 to 2007 (provided by Weisse, GKSS-Research Centre Geesthacht) to generate the representative wind conditions. The hourly wind series result from a hindcast in which a regional atmosphere model is driven with the NOAA National Center for Environmental Prediction (NCEP) and National Center for Atmospheric Research (NCAR) global re-analysis (the NCEP/NCAR global re-analysis project is using a state-of-the-art analysis/forecast system to perform data assimilation using past data to the present) in combination with spectral nudging (von Storch et al. 2000). A comparison with the limited number of available observational data shows the good quality of the model data in terms of long-term statistics such as multi-year return values of wind speed and wave heights. A detailed description of the atmosphere model and its validation are given by Weisse et al. (2009).

Wind series at five points which cover the Darss–Zingst peninsula are analyzed. A detailed statistical analysis of the wind series is described in Zhang et al. (2010a) and Zhang et al. (under review). Here, we mainly introduce the method used in the generation of representative wind series and the results of sensitivity studies which are designed to correct the representative wind series. Four seasonal classes were classified according to statistics of distribution of wind directions and wind speeds. Class 1 represents the relatively strong wind conditions for the winter season (from Oct to Feb), with the dominant wind direction from the West-South-

West; Class 2 represents a transitional season (from Mar to May) with a moderate wind strength and an East-west balanced distribution of wind directions; Class 3 represents the summer season (from Jun to Aug) with a mild wind strength and a dominant wind direction from the West-North-West; Class 4 (Sep) is a transitional season with a moderate wind strength and a dominant wind direction of West. Four representative wind series need to be generated according to the different features of the wind classes. The Weibull distribution function was used to analyze the wind strength of each class. Wind speeds of each representative series were generated by the Weibull distributed random-number generators based on the corresponding parameters of Weibull distributions of each wind class. Wind directions of each representative series were generated by the statistical results of the 50 year's data. The generated wind elements (each with a speed and direction) of each wind series were then grouped by eight wind direction sectors (N-NE, NE-E, E-SE, SE-S, S-SW, SW-W, W-NW and NW-N). A wind 'sub-group' is defined as an independent time series in which the elements have similar directions in our study. The wind sub-groups were extracted from the eight large groups mentioned above; number of wind sub-groups then has to be determined as it influences the wind duration and the wave strength in the model calculation (i.e. a large sub-group which contains a long series of wind elements with similar wind directions induces stronger waves in the model calculation than a small sub-group). As the research area is dominated by the westerly winds, we only need to analyze the division of westerly wind sub-groups. A series of sensitivity experiments was carried out to obtain the best-fit division of wind

sub-groups, which is able to induce an approximate coastline change to the measured data. Results of sensitivity experiments indicate that the calculated long-term coastline change is influenced by the division of the westerly wind sub-groups rather than by the sequence of the sub-groups. A division factor of 2 of the westerly wind sub-groups in the representative wind series produces a coastline change closer to the measured data than other factors. When the optimum division of wind sub-groups was obtained, the sub-groups were then arranged according to the short-term (hourly scale) cyclical term. The resultant representative series need to be corrected by longer-term (decadal-to-centennial) trend and cyclical terms. The yearly trend term was obtained by linear best-fit functions of the Weibull parameters of each year. Results indicate none remarkable trend term in the variation of wind strength of each class in the 50-year span. The hourly cyclical terms of each representative class were obtained by auto-correlation coefficients of wind speeds and directions with time lags from 1 to 8,760 h. Results also indicate none hourly cyclical term of each wind class. A yearly cyclical term was shown in class-averaged wind series, which indicates similarities of wind series within each class at a yearly scale. With the information of trend and cyclical terms, we are able to conclude a modelling strategy that the generated representative monthly wind series for each class, which serve as boundary inputs for the model, is repeated in every cycle of the model calculation without any trend correction. The same wind input conditions were used in the hindcast of the coastline change in the last 300 years as well as the forward projection into the next 100 years.

Statistics of the hindcast wind data from 1958 to 2007 indicate that extreme wind events frequently happen in the southern Baltic area and may play an important role in reshaping the coastline of the Darss–Zingst peninsula. Normally the definition of a storm is related to the water level variation and wind speeds. However, as only the wind data for the 50-year period is available, we define in this study a storm as a continuous time series with the maximum wind speed larger than 20 m/s, the minimum wind speed larger than 14 m/s and the duration longer than 24 h. According to this criterion, 57 storms are distinguished in the Darss–Zingst peninsula during the period of 1958–2007, of which eight storms are from the East and the rest are from the West. January and November can be described as storm months in which 31 storms happened. The distribution of storm directions indicates that the WNW is the most probable direction for a storm in this area, with a percentage of 43%. The most probable direction for an Easterly storm is the NE, with 65% of eight storms. The profile of the annual maximum wind speed indicates that wind storms happened almost every year and there is no distinct tendency in the variation of the storm strength in this 50-year period. Extreme value theory is applied to analyze the wind storms, the Gumbel distribution is

used to calculate the return periods of wind storms. According to the results of the Gumbel analysis and the distribution of wind storm directions, an annual storm from the WNW (the representative annual WNW storm is included in the representative yearly wind series in the model calculation procedure described in Fig. 12) and a once-every- n -years storm from the NE are concluded. Here, n is a number (ranges between five and ten according to statistics) which results from correction of the wind-induced wave spectrum aiming to induce coastline change similar to the measured data. Results of sensitivity studies indicate that the NE storms have significant effects on the Zingst coastline change. A return period of 5 years for the NE storms induces nearly twice coastline change as much as without NE storms in Zingst. The other parts of the research area are not very sensitive to the NE storms. These areas (Darss and Hiddensee) are mainly reshaped by long-term effects of waves and longshore currents. Wind storms from the WNW increase these long-term effects and induce about 10% of the coastline change. A return period of 5 years for the NE storm in the model produces a coastline change similar to the measured data.

5 Model application and result analysis

A digital elevation model (DEM) of the research area for the year 1696 was reconstructed based on the high-resolution bathymetric and topographic data sets measured in modern times (Meyer et al. 2008). The impacts of eustatic and isostatic processes were integrated in the reconstruction procedure. Information about the position of the historic coastline at 1696 was given by historical maps from Swedish cartographers (Curschmann 1950), which had been digitized and geo-referenced according to modern data sets. A detailed procedure of the bathymetry reconstruction is introduced in Zhang et al. (2010a). The modern-time digital elevation model for 2000 is generated from high-resolution data (50 by 50 m) provided by the Land Survey Administration Mecklenburg-Vorpommern (2006) and the Federal Maritime and Hydrographic Agency of Germany (2006). Different modules of the model were validated by comparison between the simulation results and measured time series (Zhang et al. 2010a).

The parameter settings of the long-term model are based on selected case studies and model calibration runs, in which sensitivity studies are performed to test the stability of the model with different settings. Some key settings for the model application at Darss–Zingst peninsula are presented as follows:

- (1) The open boundary hydrodynamic conditions of the local model, including the flow flux and the wave

properties, are provided by the regional model. The cohesive sediment input flux at the eastern boundary is set to zero according to the study of Christiansen et al. (2002), which indicated that the transport of cohesive sediment within the Pomeranian Bight is mainly directed to the Arkona Basin in the north and the Bornholm Basin in the east. The non-cohesive sediment input flux at the eastern boundary is also set to zero as both the model result and the study of Froehle and Dimke (2008) indicate that the net sediment transport flux is directed to the east in this area. The sediment input flux at the western boundary is also assumed to be zero as the pier of Warnemuende and the continuous dredging of the navigational channel of Rostock harbour, which are located near the western boundary of the model, block most of the sediment from being transported to the east.

- (2) Neotectonic movement in the research area is given by Harff et al. (2007). The Darss–Zingst peninsula coincides with the transition zone where there is a subsidence of -0.1 mm/year at the south-western boundary and an uplift of 0.5 mm/year at the north-easterly boundary.
- (3) The long-term sea level variation for the research area is based on the historical records as well as the results of global climate change modelling for future projection (Meyer et al. 2008).
- (4) Sediment map and classification for the model area are based on the study of Meyer et al. (2008); critical bed shear velocities of each sediment type are based on the study of Seifert et al. (2009). Initial thickness of the erodible bed is set to 10 m for all cells, which is the approximate thickness of Holocene deposits in this area. There are some glacial till elements in the Hiddensee and the Darss coast, which are covered by gravels. These sea bed elements are armoured and not easily eroded. However, these elements are still treated as sandy elements in the model since they are taking up a very small part (less than 5%) of the coastline and mostly in the deep offshore area where wave effects are not strong and sediment transport is weak.
- (5) The calculation time step of the local model is 30 s for the 2DH circulation module, 180 s for the sediment transport module. The time step of the wave calculation is dynamically determined in the wave module to ensure the numerical stability of the upwind finite difference scheme. The calculation of cliff erosion follows the time step of the wave calculation. As the sediment transport module is activated every 3 min, which is much longer than the periods of waves, the flux of cliff erosion is accumulated within the interval and serves as a source term when the sediment transport module is activated.
- (6) The nearshore storm module (XBeach) adopts the time-varying (hourly) JONSWAP spectra provided by the local model at the offshore open boundary. Time series of water level at the open boundary during the representative NE storm are also provided by the local model. Since no measurements exist to calibrate the hydrodynamics of the nearshore storm module, default values are used. The median sediment diameter is set to 0.25 mm.

Based on the reconstructed DEM, a recent sediment map, an isostatic map, an eustatic scenario for the last three centuries (Meyer et al. 2008) and validated modules, the model was applied to hindcast the coastal evolution of the Darss–Zingst peninsula from 1696 to 2000 without taking into account anthropogenic influence (Zhang et al. 2010a). The calibrated representative wind series serve as input conditions for the model. Good agreement is shown (Fig. 13) between the simulated coastline change and the measured data (the measured data is obtained by calculating the difference of coastline position in 1696 and 2000) with a RMSE= 61 m (which is about $1/5$ of the averaged coastline change of the research area for the last 300 years). Based on the validated model results, here we discuss in detail the influences of the wave processes (wave breaking and storms) on the long-term coastline change and the resultant residual transport patterns. Projected coastline change of the research area will be described in Section 5.2.

5.1 Analysis of processes driving the long-term morphological evolution

5.1.1 Wave breaking effects

Two sensitivity runs were carried out to study the effects of wave breaking (radiation stresses) on coastal evolution. The two runs are based on the same parameter setting except the consideration of wave breaking effects Eq. 3.1.2 in the 2DH circulation module. Run01 excludes the wave breaking (with both radiation stress terms equal to 0) and Run02 includes the wave breaking. Special interest is focused on the spit (Darsser Ort) and the sandy flat (Bock) shown in Fig. 14 as these two areas are most sensitive to wave dynamics in the coastal system. Figure 15 shows the calculated flow fields of these runs in two areas under a strong wind condition. In the case of the sandy flat (Bock), the only difference between the flow fields lies in the water cells adjacent to the land that are directly facing the wave incidence. Current velocity of the cells is higher under the effects of wave breaking. An increase of 30–40% in the longshore component of current velocity is modelled in Run02 compared to Run01. In the spit area (pictures at the bottom), the wave breaking causes a completely different

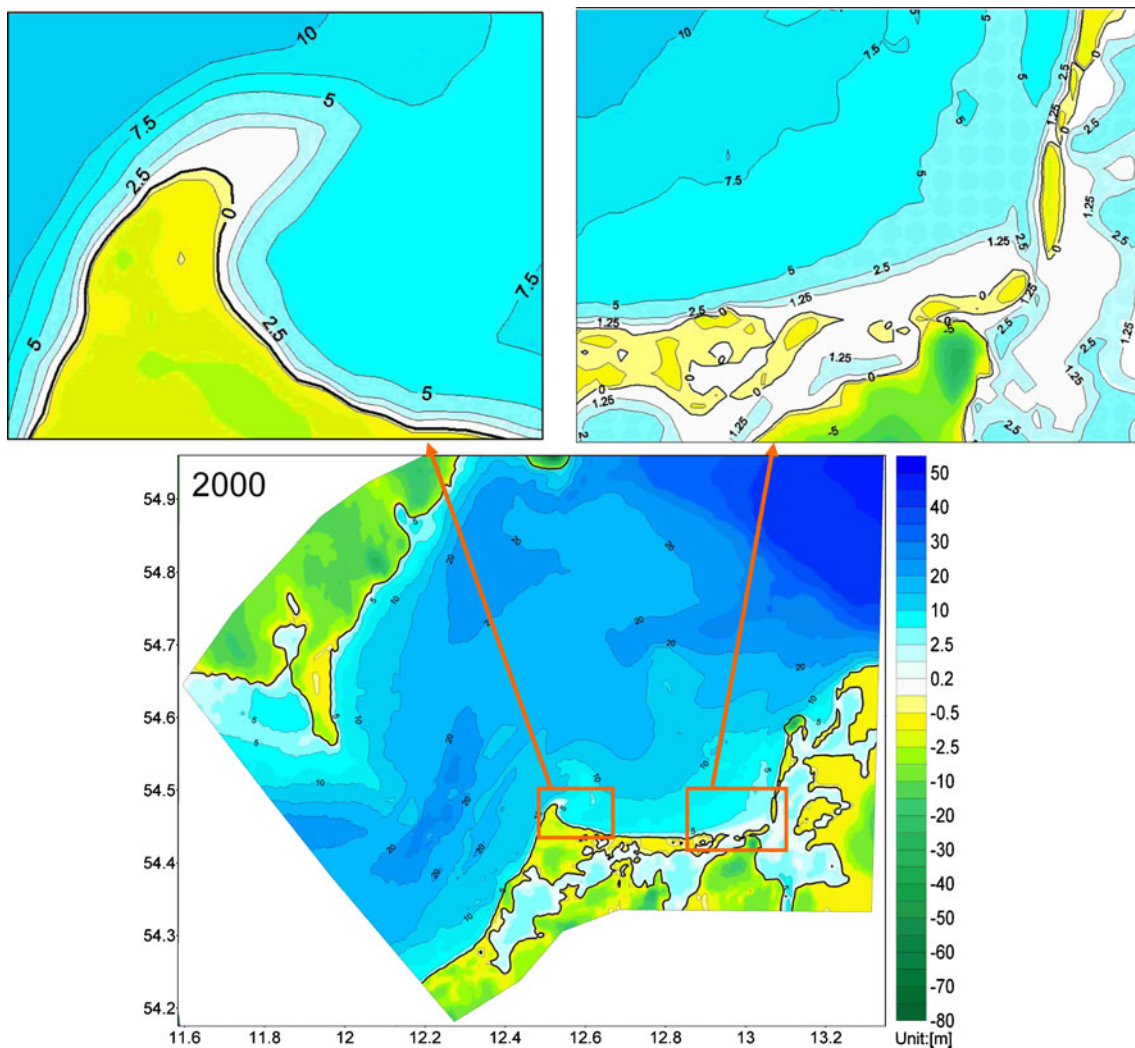


Fig. 14 Bathymetry of the Darss–Zingst peninsula in 2000. Special interest is focused on the development of two local areas (the headland ‘Darsser Ort’ and the sandy flat ‘Bock’) in the analysis of wave dynamics

flow pattern in the longshore cells at the east side. The resultant forces generated by the combination of radiation stresses, wind drag and bottom drag induce a barotropic pressure gradient in the beach area and a reverse current is formed along the beach. Such a circulation pattern is very important for the evolution of the spit, which induces a net sediment transport to feed the growth of the east side of the spit. Based on the reconstructed DEM for the study area in 1696, a 20-year bathymetrical change from 1700 to 1720 is simulated in two runs to study the evolution of the Darss–Zingst peninsula under the long-term effects of wave breaking in this period. Differences between the results are shown in Fig. 16. At the Darss coast, more sedimentation in the offshore area is modelled in Run02 under the wave breaking effects, as well as more erosion at the coastline area. This is plausible as the wave breaking not only increases the longshore current velocity but also enhances the bottom friction and entrains more sediment

in the water column. Large amounts of sediment from erosion of the coastline area are deposited in the offshore area where wave effects are relatively weak; the rest is carried by the longshore currents. Such wave breaking-induced effect is more evident in the spit area as it serves as a convergence for the sediment transported by the longshore currents from both sides. Less coastline erosion at the west side of the spit is modelled in Run02 as it is partly compensated by deposition of sediment. This coincides with the rate of the local coastline erosion in the last 300 years, which is about 0.9 m/years. Another phenomenon caused by long-term wave breaking effects that should be noted is the development of the east side of the spit. This can be partly explained by the flow pattern indicated in Fig. 15. The wave breaking-induced flow helps to distribute the sedimentation in a broader area along the east side of the spit, thus causing a faster development of the area than in Run01. Wave breaking is also responsible for trans-

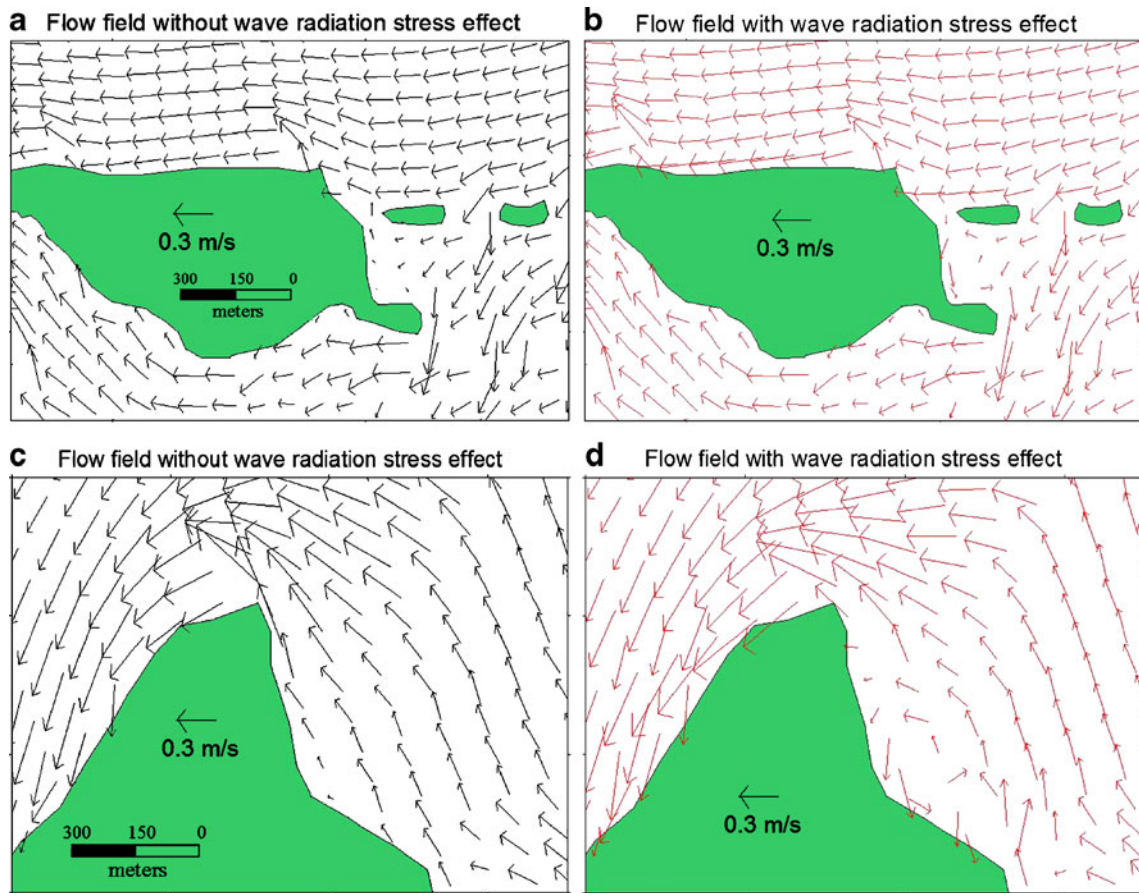


Fig. 15 Comparison between the flow fields with and without wave breaking effects. Instant wind speed is 16 m/s, and wind direction is North-East

porting more sediment from the west side to feed the development of the east side of the spit. About 40% more sedimentation is modelled in Run02 compared to Run01. This is also validated by the fast growth of the east side of the spit which is about 3 m/year towards the northeast during the last 300 years. Along the Zingst coast, wave breaking causes similar sediment transport pattern to that along the Darss coast, and contributes to the fast development of the Bock area. Wave breaking also helps to ‘pump’ more sediment into the inner lagoon through the channel between Hiddensee Island and Zingst, causing substantial deposition in this area.

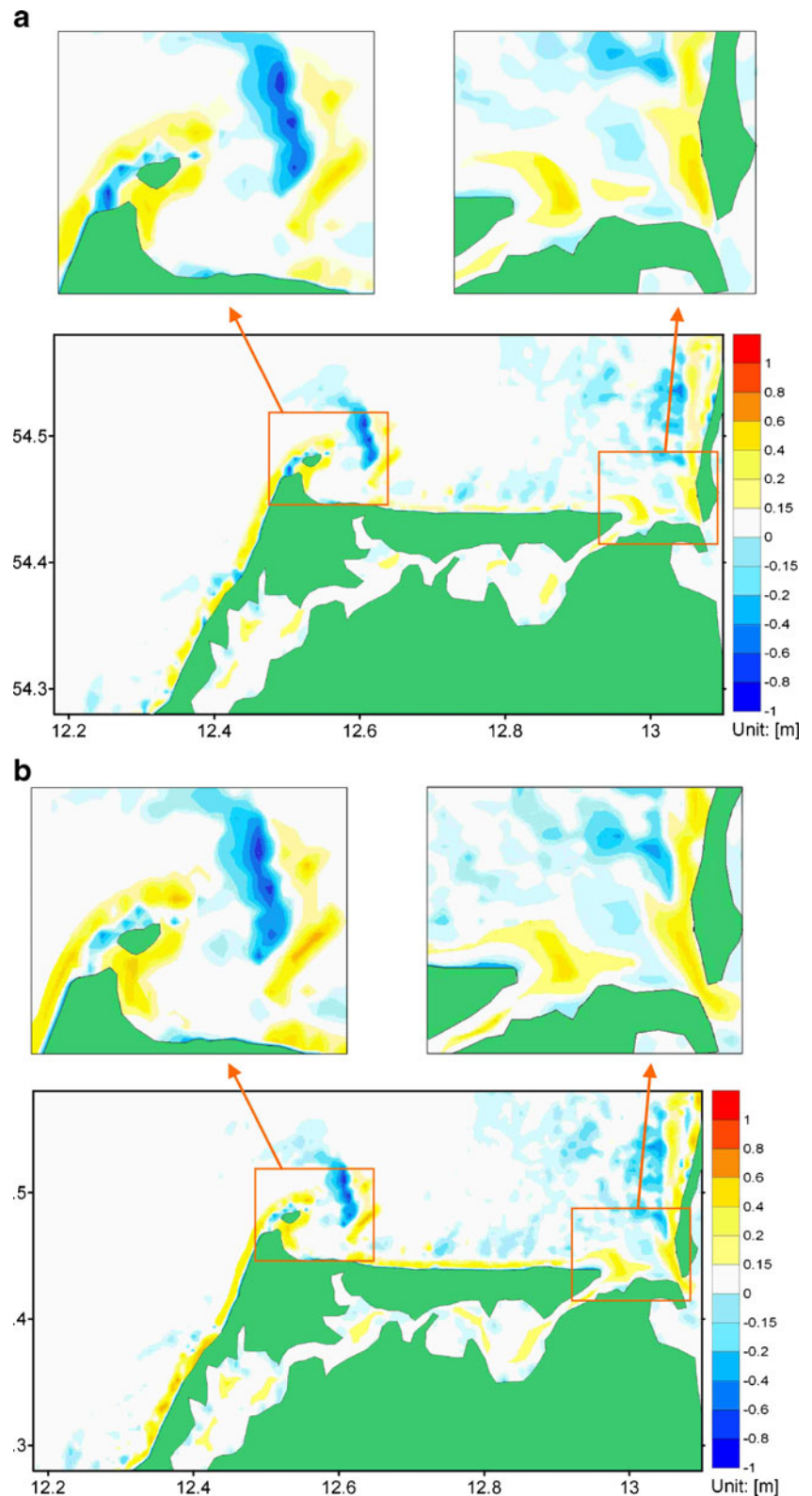
5.1.2 Storm effects

As indicated by the model results, the long-term effect of wave dynamics (shoaling, breaking and longshore currents) is the dominant factor influencing the evolution of the Darss and Hiddensee coastline. However, such long-term wave effects cannot fully explain the coastline change of the Zingst area in the last centuries, which is about 1 m/year on average and much faster than the average rate of the

coastline change in Darss (around 0.5 m/year). The terrain of the Darss–Zingst peninsula (Fig. 14) provides a natural sheltering effect for the Zingst coast from the dominant westerly wind-induced waves, thus the fast coastline change of Zingst cannot be caused by the dominant western wave dynamics. Sensitivity results described in Section 4 indicate that the morphological evolution of Zingst is a combination of effects of short-term storms (especially the Eastern storms) and long-term wave dynamics.

Different from the bathymetrical change driven by long-term hydrodynamics, the storm-induced bathymetrical change is often temporary and would be levelled after a certain time period (which is called ‘recovery’). This yields for most wet areas which are permanently under the effects of currents and waves, but for the areas which are only affected by high water levels caused by storms, the storm-induced change is permanent and cannot be recovered. Two kinds of representative storms, one is high-frequency (once per year) from the West-North-West and the other is low-frequency (once every 5 year) from the North-East are concluded through statistical analysis of 50-year wind data and sensitivity studies which were introduced in the

Fig. 16 **a** Calculated bathymetrical changes without wave breaking effects after a 20-year simulation; **b** Calculated bathymetrical changes with wave breaking effects after a 20-year simulation. Positive number indicates deposition and negative number indicates erosion



previous section. The representative storms generally reflect the typical storm conditions (direction, duration, wind strength, significant wave height and wave-induced run-up) in the southern Baltic Sea. Model results indicate that

these two kinds of storms have different effects on the coast. The WNW storm is not able to cause a high water level due to insufficient water supply and wind fetch, which is restricted by the morphology of the south-western Baltic

Sea. The calculated highest water level in the Darss–Zingst area is 0.6 m (above mean sea level) and the maximum wave-induced run-up is 1.6 m during a representative WNW storm. However, the highest water stand and maximum wave-induced run-up happen at different places (the highest water stand happens at the Bock area while the maximum wave-induced run-up happens at the Darss coast), thus do not overlap. Such a limited water stand and wave run-up restricts the storm effects mostly in the nearshore area (Fig. 17, right panel). Wave breaking mainly happens in the coastline area of Darss, the eastern part of Zingst and Hiddensee, causing significant sediment transport in these areas. The WNW storm also has a significant influence on the offshore area between Zingst and Hiddensee as the water depth of this area is within 10 m. The calculated bathymetrical change after a WNW storm (Fig. 18, right panel) indicates that the most remarkable change happens in the spit area, with strong erosion at the spit on the magnitude of centimetres and deposition in the deeper area east beside the spit. At Zingst and Hiddensee, the WNW storm drives the sediment towards the East in the offshore area and swashes the coastline, causing deposition

in a strip area along the coast of Hiddensee and the channel between Bock and the southern tip of Hiddensee. The WNW storm does not cause much change along the major part of Zingst as this area is sheltered by the spit and the incident angle of waves is too large to induce significant wave breaking (Fig. 17, right panel).

The NE storm has very different effects compared to the WNW storm as it not only induces strong waves in the Zingst area but also causes a high water level at the same place (Fig. 17, left panel). The calculated highest water stand is 1.8 m and the maximum wave run-up is 1.5 m along the Zingst coast during a NE storm. Such overlapping effect makes large part of the Zingst coast inundated by water during a NE storm. Because of the high water stand, the NE storm has limited effects in the offshore area and mainly influences the Zingst coast which is directly facing the wave incidence. Model results indicate that the NE storm-induced change is mainly limited to the Zingst coast and the spit area. The Zingst area suffers erosion along the coastline and inundated areas, which is on the magnitude of centimetres. The erosion in most parts of Zingst cannot be recovered by long-term effects of waves and currents as

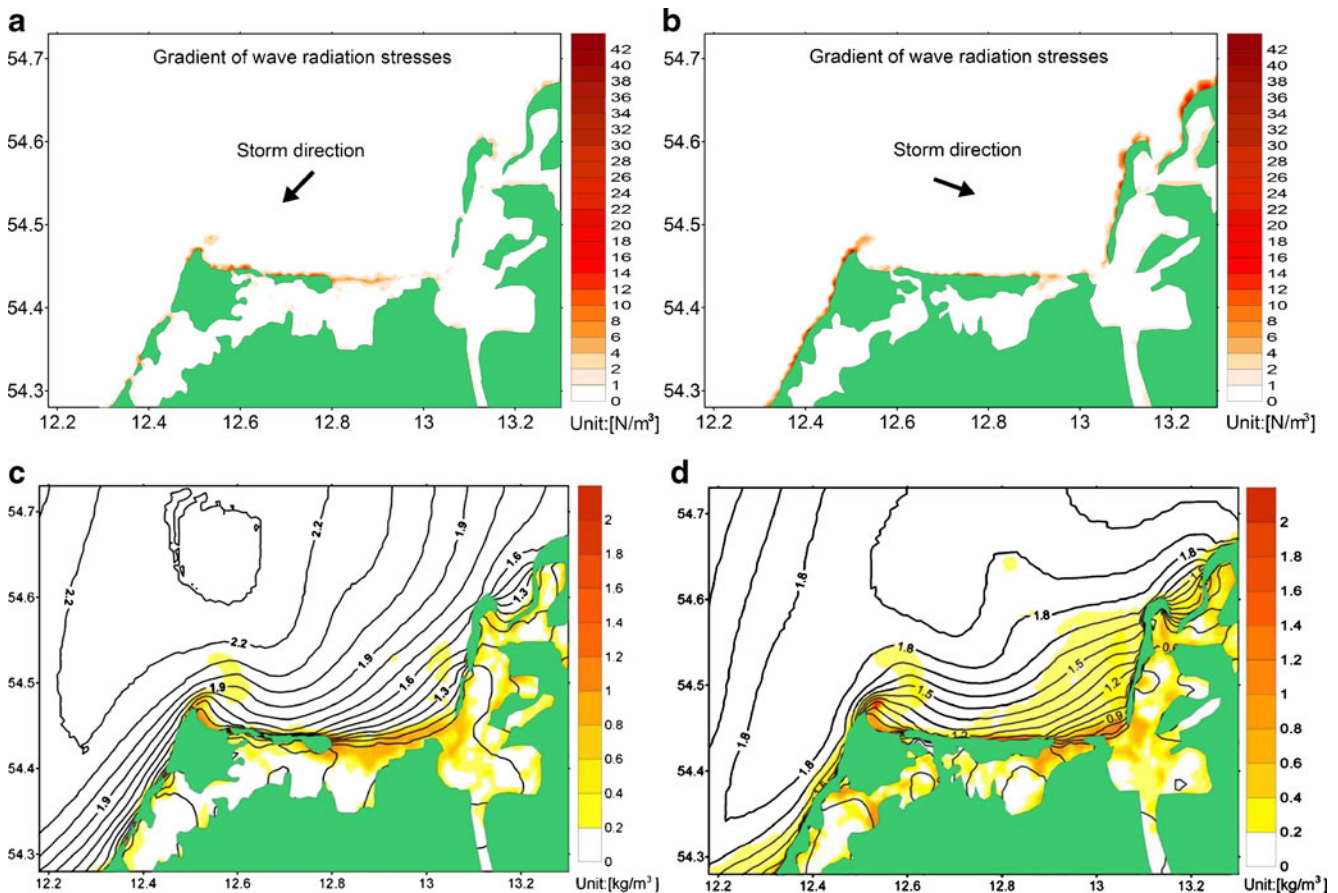
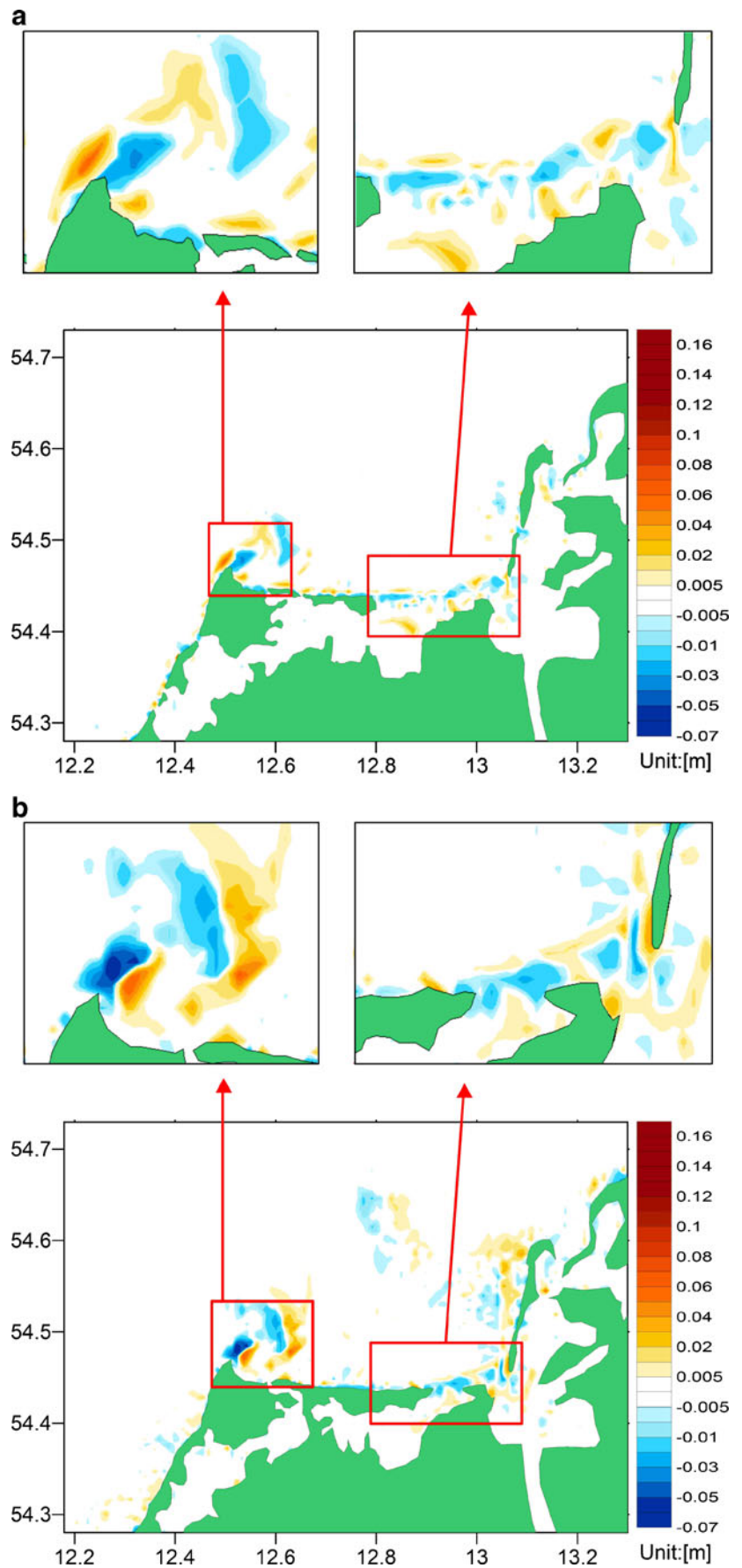


Fig. 17 a and b Gradients of wave breaking-induced radiation stresses during the representative storms. c Distribution of significant wave height (solid lines) and suspended sediment concentration during a representative

north-easterly storm; d distribution of significant wave height (solid lines) and suspended sediment concentration during a representative WNW storm. Instant wind speed is 20.5 m/s for all cases

Fig. 18 **a** Simulated bathymetrical change after a representative NE storm; **b** Simulated bathymetrical change after a representative WNW storm



these parts are only affected by high water level during NE storms. The continuous sea-level rise (in the past and coming centuries) causes increasing storm-induced change at higher parts of the coast. This storm-induced erosion doubles the rate of coastline retreat which is solely caused by the long-term effects of waves in the Zingst area. This effect can be used to explain the fast coastline change of Zingst during the last 300 years. In the spit area, the NE storm also causes erosion at the spit and deposition at its west side.

Simulation results of two kinds of representative storms seem (Fig. 18) to indicate that the storms act as a hindering factor for the growth of the spit. However, storms also serve sediment supply for the long-term growth of the spit, especially for its east side. Although being eroded during storms, the growth of the spit is compensated very soon by abundant sediment supply carried by longshore currents under mild weather conditions. Based on the simulations results, we conclude that storms are an important factor influencing the evolution of the Darss–Zingst peninsula.

5.1.3 Residual flow and sediment transport

The residual flow field and sediment transport flux in the research area are calculated by the representative yearly climate conditions (Fig. 19). The residual results generally show the prevailing transport patterns in this area, which are dominated by the westerly winds. However, we can still find some differences between the residual flow field and the sediment transport flux field by comparing these two pictures. The residual sediment transport flux is restricted to a narrow zone with a width less than 1,000 m along the Darss coast and shows a discontinuous pattern (which is not shown in the residual flow field), with some discrete large fluxes directed offshore. This indicates the cross-shore transport as another important sediment transport pattern along the Darss coast. The cross-shore sediment transport in the model is induced by two factors: the longshore variation of the radiation stresses and the bathymetry. The main difference between the residual flow field and sediment transport flux field lies in the spit area. The residual flow and sediment transport flux both converge at the spit, after that the residual flow is directed to the upper east side of the spit, while the residual sediment transport flux is directed to the upper west side. Such difference indicates that the residual sediment transport flux is not completely determined by the residual flow. Another interesting difference is that the residual sediment transport flux along the Zingst coast has a compensation pattern in the further offshore area which is directed opposite to the main transport direction along the coastline. Such differences between the residual flow field and the sediment transport flux field may be explained by the effects of easterly winds and

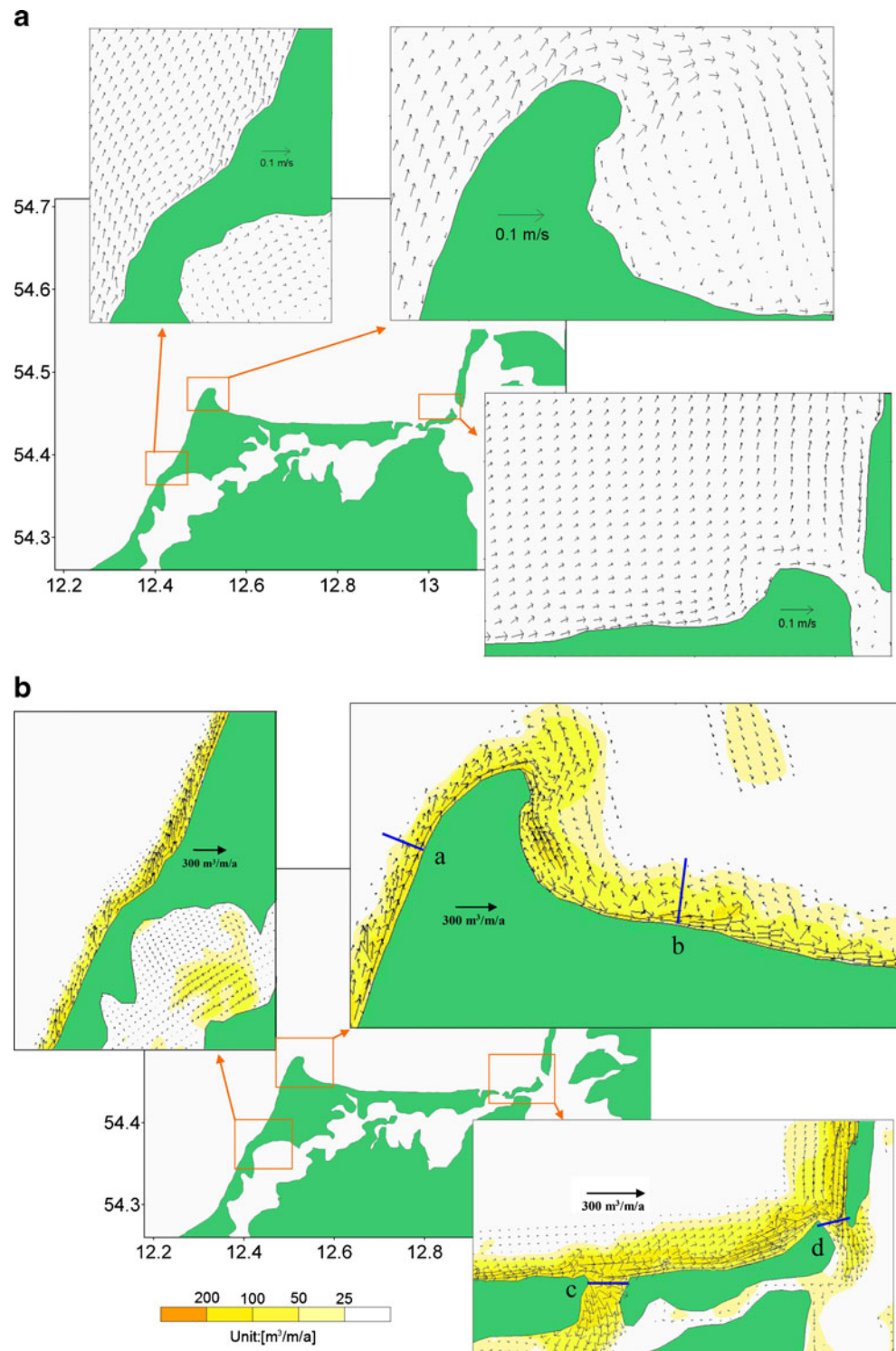
westerly winds on the sediment transport pattern in this area. The westerly winds are not able to induce significant sediment transport on the east side of the spit and the Zingst part close to the spit due to the sheltering effects of the terrain, which restricts the westerly wind-induced wave breaking in a narrow surf zone in this area. In contrast to the westerly winds, the easterly winds have a direct and stronger effect in this area with wave breaking happening further offshore, thus are able to induce significant sediment transport towards the west. At a longer time scale (annual), the westward sediment transport along the coastline in this area is counterbalanced by the eastward transport which is induced by the dominant westerly winds, but such counteracting effects mainly happens in a narrow surf zone area where the waves induced by westerly winds break, and in the further offshore area where the strong easterly wind-induced waves start to break, the westward sediment transport is not fully counterbalanced. The residual effects caused by differences between the westerly wind-induced waves and the easterly wind-induced waves may also help to explain the formation and evolution of the underwater sand body in the spit area.

Along the Zingst coast to the Bock Island, the sheltering effects of terrain become weak and the westerly wind-induced sediment transport pattern gradually dominates. The residual sediment transport flux field corresponds with the residual flow field in the Bock area. The residual sediment transport flux field indicates two inlets adjacent to the Bock Island as depositional areas. However, the main sources for deposition in these two inlets are different: the sediment source for the west inlet is mainly from the Zingst area; while sediment from the Hiddensee Island and the Zingst area both serve as important sources for the east inlet. The calculated residual sediment transport flux is about 180,000 m³/year (toward the northeast) at a coastal section (Section a) along Darss; about 70,000 m³/year (toward the east) at a coastal section (Section b) that is located in the Zingst part close to the spit. Hence, about 110,000 m³/year of sediment is deposited in the spit area to feed its growth. About 25,000 m³/year of sediment is transported into the west inlet (Section c) of the Bock Island and about 20,000 m³/year of sediment into the east inlet (Section d), which gradually fills these inlets in the twenty-first century. The calculated residual sand flux in the model is in good agreement with studies of Froehle and Dimke (2008).

5.2 Model projection

Based on a successful hindcast of the coastline change of the Darss–Zingst peninsula for the last 300 years, the model is used to project the evolution of the same area for the next 100 years without consideration of anthropogenic influen-

Fig. 19 **a** Residual flow field calculated by the representative yearly wind conditions; **b** residual sediment transport flux calculated by the representative yearly wind conditions

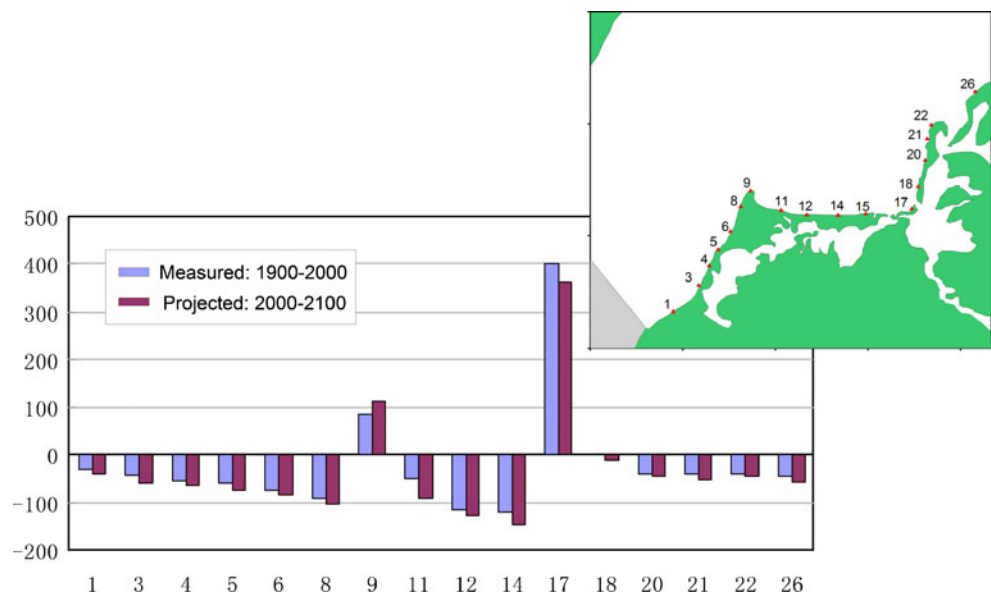


ces. Coastal engineering work has provided additional protections for the Darss–Zingst coastline since the last century (Froehle and Kohlhasse 2004), and will continue in the future. Such anthropogenic influence will make our model projection results less reliable. However, this does not mean that model projection without anthropogenic factors is useless. On the contrary, projection results can

help to make the coastal management more efficient as they indicate the possibility of coastline change under the presumed climate scenario, thus providing useful information for the coastal engineering work.

The representative wind conditions, neotectonic movement and sediment properties in the projection run are following the same settings as the hindcast run. The sea-level change in the

Fig. 20 Comparison between the measured coastline change in the twentieth century and the projected results in the next 100 years



projection run is following the study of Meyer et al. (2008), which is about 2 mm/year in the next 100 years. This rate is twice as much as the rate in the last three centuries.

5.2.1 Morphological change

Except the spit and the Bock area, other parts of the Darss–Zingst peninsula will be facing continuous erosion in the next 100 years according to the projected results (Fig. 20). An increment of 10–15 m in the coastline retreat at the Darss coast is projected comparable to the change in the twentieth century, while the coastline change of Zingst would be more drastic with an increment of 20–30 m. This is due to the effects of accelerated sea-level rise.

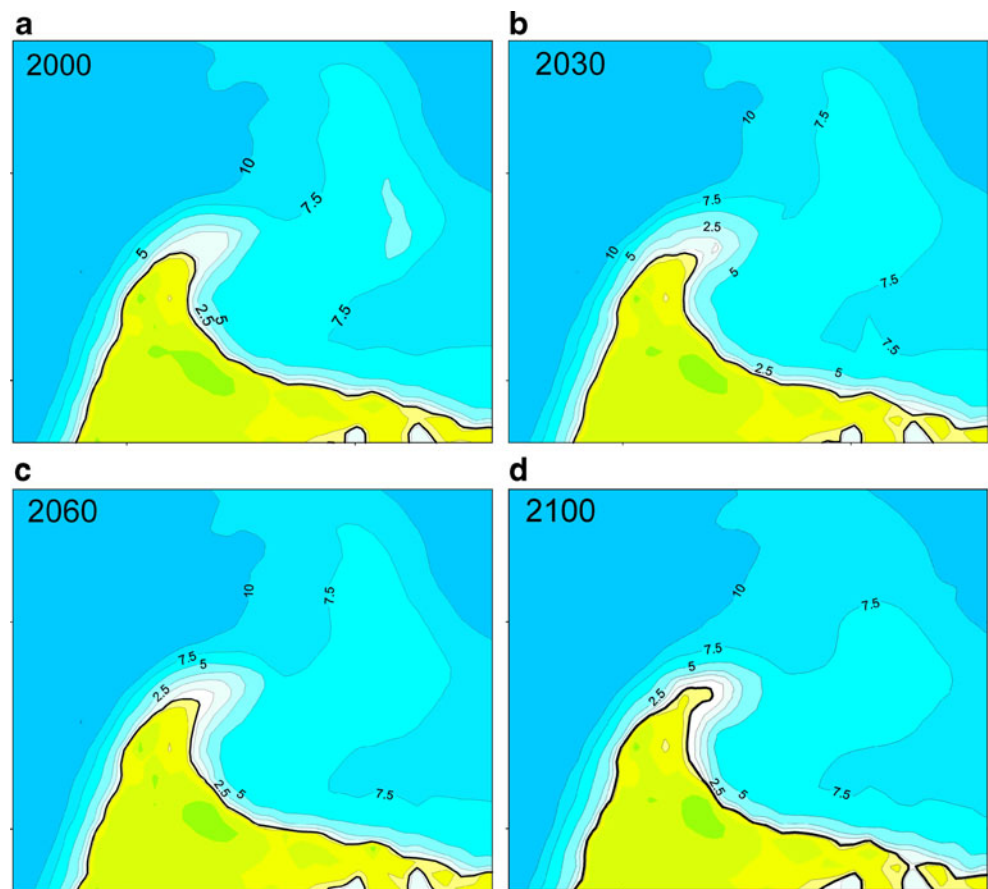
The projected evolution of the spit is shown in Fig. 21. The growth of the spit is projected to occur at a high rate due to abundant sediment supply. There are several phases of growth of the spit. First is the development of the sand body in front of the spit in the first 30 years. The sand body is not completely attached to the spit but with some part separated, which is due to the erosion at the west side of the spit (as shown in Fig. 9, right panel). As the sand body continues to grow, the separated part would attach the spit from the east side between 2030 and 2060 (Phase 2). In Phase 3 from 2060 and 2100, a part of the sand body would become land due to the neotectonic movement and its growth is slowed down. The slow-down of the spit's growth is partly due to the relatively deep water environment in front of it; and partly due to the counterbalancing effect of sea-level rise. The west side of the spit is facing erosion continuously in spite of the growth of its east side. Such phenomenon makes the spit 'shifting' towards the north-east. The maximum projected 'shift' (distance between the tip position in 2000 and 2100) of the spit is about 250 m.

The projected evolution of the Bock area (Fig. 22) has a more complex form compared with the evolution of the spit. The morphological evolution of the Bock area is not only determined by the sediment supply from outside areas (Zingst and Hiddensee), but also influenced by the hydrodynamics controlled by the two inlets. The west inlet serves as the main intermediate for water exchange between the inner lagoon and the outer sea. However, this inlet cannot play an efficient role in connecting the two water bodies due to the limited accommodation space at its inner side, which is squeezed by high lands. Along with filling of the limited accommodation space in the next 100 years when abundant sediment supply is provided, the west inlet would gradually close. New and more efficient inlets would be opened in other parts of Zingst (Zhang et al. under review). Different from the west inlet, the east inlet has a longer life span as this inlet acts more efficiently to connect the inner water body with the outer sea. The accommodation space at the inner side of the east inlet is large enough for the incoming sediment, and active hydrodynamics in the inlet help to maintain the water channel. Large amounts of sediment are deposited in the sandy flat between these two inlets, causing an increased land area, which would attach to the Zingst coast after the close of the west inlet.

5.2.2 Coastal profile change

Projected evolution of three typical coastal profiles along the Darss–Zingst peninsula is shown in Fig. 23. Each profile has a unique response to sea-level rise. Profile A1 has a relatively steep gradient of 0.83°. At such a steep gradient and under the effect of continuous sea-level rise, sediment at Profile A1 is moved off- rather than onshore, causing erosion in the upper part and deposition in the lower part. The rate of

Fig. 21 Projected evolution of the headland (Darsser Ort) in the next 100 years



change at Profile A1 is fast in the first 30 years, and then gradually slows down. This is due to the deposition at the lower part which reduces the gradient and causes more wave energy dissipation before their arrival at the coastline. By comparing the volume of erosion at the upper part with the volume of deposition at the lower part, we find that not all the eroded sediment is directly deposited offshore. About 30% of the eroded sediment at Profile A1 is transported away, mostly north-eastward to the spit area. A closure depth (bathymetrical change < 0.05 m/100 years) of 12 m is modelled at Profile A1, which is about 1200 m offshore. Profile A2 at the Zingst coast has a relatively mild gradient (0.39°) compared with A1, however, this mild gradient allows more variable profile changes under the effect of sea-level rise. Although being continuously eroded at the upper part, Profile A2 never seems to attain equilibrium in the next 100 years. The first 60 years is a ‘smoothing’ period for Profile A2 as more deposition at the lower part than erosion at the upper part is modelled, but such ‘smoothing’ effect is eliminated in the coming 40 years (2060–2100) by stronger erosion at the upper part of the profile. This change in Profile A2 may be caused by the gradually decreased sediment supply from the spit area, where more and more sediment is trapped in the deep water along with the growth of the spit (as shown in Fig. 21). The change of Profile A3 has a quite

different process compared with the other two profiles. The upper part of this profile is characterized by sedimentation rather than erosion. The gradient of Profile A3 is very steep in the first 200 m (1.4°) and then dramatically decreases in the following several kilometres. Such a steep gradient is caused by dredging of the channel between Bock and Hiddensee, but this dredging effect will be eliminated (without further anthropogenic influences) in the next 60 years with fast deposition in this area. Model results indicate that the sediment from further offshore area serves as an important source for deposition in the upper part of Profile A3. After fast change in the first 60 years, Profile A3 seems to attain equilibrium during 2060 and 2100. A large fraction of wave energy is dissipated in the shallow offshore areas of Profile A3, causing very limited erosion at the coastline, which is merely 16 m from 2000 to 2100 according to the simulation results.

6 Discussion and summary

6.1 New features of the modelling methodology

In order to solve the problem of boundary input for the long-term model, the concept of representative wind series

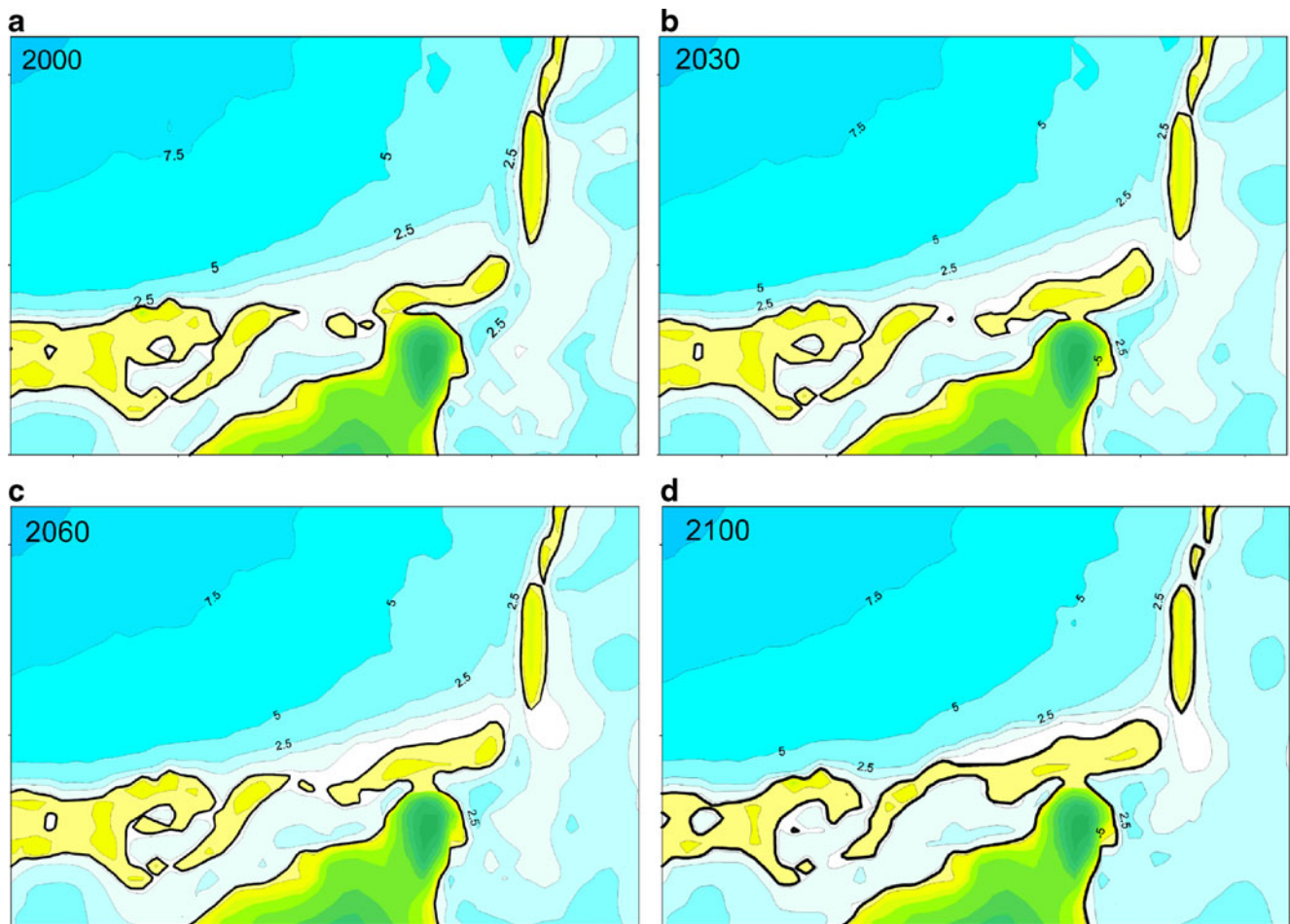


Fig. 22 Projected evolution of the sandy flat (Bock) in the next 100 years

is introduced in our study. This is different from some previous studies (Cayocca 2001; Jimenez and Arcilla 2004) which use the representative wave series. The use of representative wind series has two advantages compared with representative waves: (1) the winds are quite similar at different sites within a local area (e.g. the Darss–Zingst peninsula) while the waves are not. Thus a uniform representative wave series for the whole area is not able to reflect the influence of the bathymetry and topography on the wave dynamics. On the other hand, it would be a time-consuming work to specify different representative wave series for different areas. One advantage of the use of the representative wind series is that it enables the model to calculate the wave properties at different sites (rather than specify them) and to reflect the wave spectrum with different directions and strengths in the research area. The calculated wave spectrum from the representative wind series shows good agreement with the measured wave spectrum (as shown in Fig. 2); (2) the rules of the short-term wind storms such as strength, direction, duration and return periods are easier to study in a direct way by

statistical analysis of the historical wind data. The use of representative wind series is also easier to reflect the influence of climate change on the main driving forces of the hydrodynamic system in the Baltic Sea.

The coastline (cliffs and sandy beaches) erosion is calculated in a relatively simple way in our model, although it is much more complicated in nature. The treatment of the sandy beaches as ‘dune cliffs’ enables a simplification of the mechanisms controlling the coastline erosion and calculation of the coastline erosion on a relatively large spatial scale. This method proves to be an efficient way to improve the efficiency of the long-term model without causing significant bias between the hindcast result and the measure coastline change during the last 300 years. However, the validity of this method still needs to be further studied by the application of the model to other coastal cases where small-scale cross-shore processes are dominant for the coastline change.

The methods (‘online approach’ and ‘straightforward extrapolation’) used for the bathymetrical update in the model prove to be an efficient way in accelerating the long-

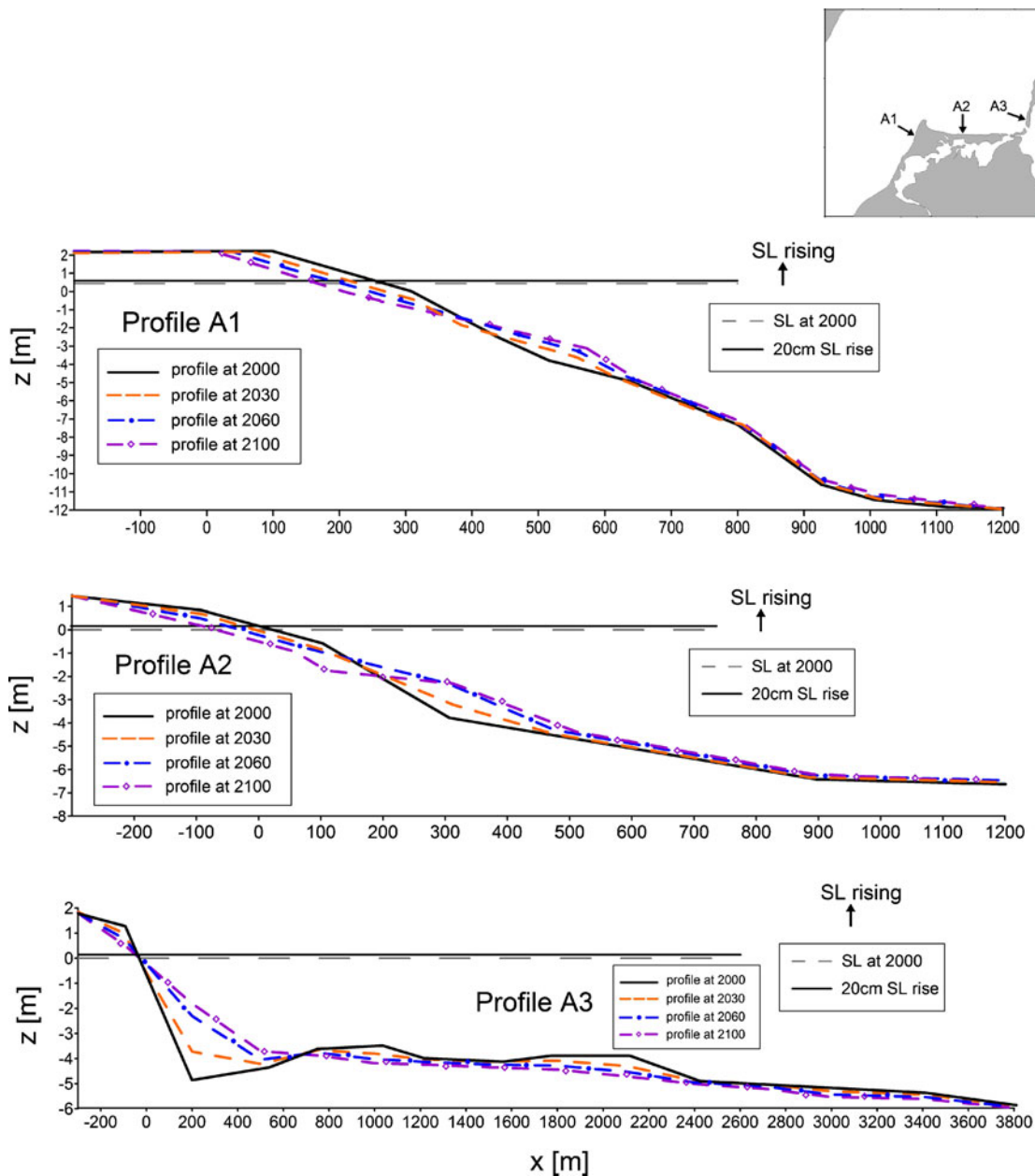


Fig. 23 Projected evolution of three coastal profiles of the Darss–Zingst peninsula in the next 100 year

term calculation without causing any instability. ‘Partly freezing’ the suspended sediment transport in the shallow water cells (<1.5 m) under mild wind conditions seems to be arbitrary, but this assumption in the model does not induce remarkable bias between the simulation results and the measured data due to the fact that bed-load/erosion is the main transport process in the nearshore shallow water areas of the southern Baltic Sea (Schwarzer and Diesing 2003).

The separation of calculation of short-term hydrodynamics (storm) and long-term hydrodynamics in our model is an efficient way to save CPU time. Cross-shore transport is the

main sediment transport pattern during the short-term storms, and small-scale processes are mainly responsible for that, which need to be resolved in a high-resolution grid. The resolution of the local grid, in which long-term morphological evolution is calculated, is determined by sensitivity studies. Although a full three-dimensional high-resolution grid is the best choice to resolve some small-scale wave processes such as undertow, wave asymmetry and rip current, a resolution of 100 m for the nearshore area in a two-dimensional vertically averaged grid proves to be able to produce reasonable good simulation results. This suggests that the meso-to-large-scale depth-averaged processes (wind-driven circulation, wave-

induced longshore currents and return flow induced by longshore variation of radiation stresses and bathymetry), rather than small-scale vertical processes, act as the main long-term hydrodynamic factor driving sediment transport in the Darss–Zingst peninsula.

6.2 Shortcomings and future work

The process of transition for the shallow water cells to terrestrial ones is described relatively simply in our model even with errors within an acceptable range. This is because that only a small part of the area is undergoing such siltation process. However, this approach might cause non-negligible problems if longer-term (such as a millennium-scale) evolution of a barrier island is modelled, because a large fraction of the area may undergo a series of transition phases from land to water or from water to land. A disadvantage of the model is that no aeolian effects are considered, which are responsible for building the sand dunes. Without any sand-dune protection, the newly formed land cells would be easily eroded by strong waves during storms. The fragility of these terrestrial cells can induce continuous transitions between land and water in the model and errors can pile up to dominate the results. Thus, the processes driving the transition between land and water need to be further studied when the model is applied to a longer-term simulation.

Another shortcoming of the model is the error generated in the cliff erosion module. A method is used to solve the fluctuation problem, but the overestimated erosion is smoothed rather than eliminated. The calculated coastline change in the last 300 years generally fits the measured data without significant bias, which proves the efficiency of the method applied at this time scale; however, this method needs to be evaluated more carefully when the model is applied to a longer time span such as millennia.

In order to overcome the shortcomings of the model, our future work will focus on the incorporation of the aeolian processes into the model and improvement of the calculation of suspended sediment transport in the shallow water area (< 1.5 m) and the corresponding bed-level update strategy. A better consideration of the coastline erosion in the model is also a target of our future work.

6.3 Summary

Despite several shortcomings of the model, the methodology described in this study proves that the process-based model, with combination of a series of modelling strategies in which multi-scale concepts and ‘reduction’ techniques are implemented, is an efficient tool to study long-term coastal evolution under the effects of climate change. Two factors, long-term wave dynamics (wave breaking and long-

shore currents) and short-term storms, are indicated as the dominant factors controlling the morphological evolution of the Darss–Zingst peninsula.

Acknowledgements We thank the reviewers for their valuable comments. The historical wind data (1958–2007) of the Baltic Sea were kindly provided by Dr. R. Weisse. The simulations were carried out at the supercomputing facilities of the MPI-IPP (Max-Planck-Institute for Plasma Physics) in Greifswald and Garching, Germany. The research work is supported by the SINCOS project. One author (Zhang, W.Y.) is supported by a scholarship offered by the China Scholarship Council (CSC).

References

- Bailard JA (1981) An energetics total load sediment transport model for a plane sloping beach. *Journal of Geophysical Research* 86 (C2) 10:938–954
- Bouws E, Guenther H, Rosenthal W, Vincent CL (1985) Similarity of the wind spectrum in finite depth water I. Spectral form. *J Geophys Res* 90:975–986
- Budetta P, Galiotta G, Santo A (2000) A methodology for the relation between coastal cliff erosion and the mechanical strength of soils and rock masses. *Eng Geol* 56:243–256
- Cayocca F (2001) Long-term morphological modeling of a tidal inlet: the Arcachon Basin, France. *Coast Eng* 42:115–142
- Christiansen C, Edelvang K, Emeis K et al (2002) Material transport from the near shore to the basinal environment in the southern Baltic Sea: I: processes and mass estimates. *J Mar Syst* 35:133–150
- Curschmann F (1950) Matrikelkarten von Vorpommern: 1692-1698, Karten und Texte, 1. Carl Hinstorff Verlag, Teil.-Rostock
- Dastgheib A, Roelvink JA, Wang ZB (2008) Long term process-based morphological modelling of the Marsdiep tidal basin. *Mar Geol* 256:90–100
- de Vriend HJ, Copabianco M, Chesher T, De Swart HE, Latteux B, Stive MJF (1993a) Long term modelling of coastal Morphology. *Coast Eng* 21:225–269
- de Vriend HJ, Zyserman J, Nicholson J, Roelvink JA, Pechon P, Southgate HN (1993b) Medium term 2DH coastal area modelling. *Coast Eng* 21:193–224
- Diesing M, Furmanczyk K, Hanson H, Niedermeyer RO, Pruszk Z (1999) Present fluxes of inorganic matter in Pomeranian Bay. 3rd BASYS Final Conference, Institut für Ostseeforschung Warnemünde, Warnemünde. Available at: <http://www.io-warnemuende.de/Projects/Basys/bio/con3/con3top.htm#T2-10>
- Dissanayake DMPK, Roelvink JA (2007) Process-based approach on tidal inlet evolution-Part 1. In: Janssen D, Hulscher (eds) River, Coastal and Estuarine Morphodynamics: RCEM 2007. Taylor & Francis Group, London, ISBN 978-0-415-45363-9
- Donelan MA (1977) A simple numerical model for wave and wind stress application. Report, National Water Research Institute, Burlington, 28 pp
- Emeis K, Christiansen C, Edelvang K et al (2002) Material transport from the near shore to the basinal environment in the southern Baltic Sea: II: synthesis of data on origin and properties of material. *J Mar Syst* 35(3–4):151–168
- Fagherazzi S, Overeem I (2007) Models of deltaic and inner continental shelf landform evolution. *Annu Rev Earth Planet Sci* 35:685–715
- Froehle P, Dimke S (2008) Sediment Transport at the Coast of Mecklenburg-Vorpommern, Germany. In: Smith JM (ed.) Proceedings of the 31st international conference on Coastal Engineering, Hamburg, Germany, 3. pp 2471–2480

- Froehle P, Kohlhas S (2004) The role of coastal engineering in integrated coastal zone management. In: Schernewski G, Löser N (eds) *Managing the Baltic Sea, Coastline Reports 2*, ISSN 0928-2734 S. 167-173
- Glenn SM, Grant WD (1987) A Suspended Sediment Stratification Correction for Combined Wave and Current Flows. *J Geophys Res* 92(C8):8244–8264
- Grant WD, Madsen OS (1979) Combined wave and current interaction with a rough bottom. *J Geophys Res* 84:1797–1808
- Harff J, Lemke W, Lampe R, Lüth F, Lübke H, Meyer M, Tauber F, Schmölcke U (2007) The Baltic Sea Coast-A model of interrelations among geosphere, climate, and anthroposphere. In: Harff J, Hay WW, Tetzlaff DM (eds.) *Coastline Changes: Interrelation of Climate and Geological Processes*. The Geological Society of America, Special Paper, 426:133–142
- Hasselmann K, Barnett TP, Bouws E, Carlson H, Cartwright DE, Enke K, Ewing JA, Gienapp H, Hasselmann DE, Kruseman P, Meerburg A, Mueller P, Olbers DJ, Richter K, Sell W, Walden H (1973) Measurements of wind-wave growth and swell decay during the Joint North Sea Wave Project (JONSWAP). *Deutsche Hydrographische Zeitschrift, Ergänzungsheft*, A8, 12, p 95
- HydroQual, Inc (2002) *A Primer for ECOMSED version 1.3. (computer program manual)*: Mahwah, New Jersey, HydroQal, Inc.
- Jimenez JA, Arcilla AS (2004) A long-term (decadal scale) evolution model for microtidal barrier systems. *Coast Eng* 51:749–764
- Jones OP, Petersen OS, Hansen HK (2007) Modelling of complex coastal environments: Some considerations for best practise. *Coast Eng* 54:717–733
- Kliewe H (1995) Zeit- und Klimamarken in Sedimenten der südlichen Ostsee und ihrer Vorpommerschen Boddenküste. *J Coas Res Special Issue* 17:181–186
- Kolp O (1978) Das Wachstum der Landspitze Darsser Ort. *Petermanns Geogr Mitt* 122:103–111
- Kuhrts C, Fennel W, Seifert T (2004) Model studies of transport of sedimentary material in the western Baltic. *J Mar Syst* 52:167–190
- Lampe R (2002) Holocene evolution and coastal dynamics of the Fischland Darss Zingst peninsula. *Greifswald Geogr Arb* 27(D1):155–163
- Lampe R (2005) Lateglacial and Holocene water-level variations along the NE German Baltic Sea coast: review and new results. *Quatern Int* 133–134:121–136
- Latteux B (1995) Techniques for long-term morphological simulation under tidal action. *Mar Geol* 126:129–141
- Lesser GR, Roelvink JA, van Kester JATM, Stelling GS (2004) Development and validation of a three-dimensional morphological model. *Coast Eng* 51(8–9):883–915
- Longuet-Higgins MS, Stewart RW (1964) Radiation stresses in water waves, a physical discussion with applications. *Deep-Sea Res* 11:529–562
- Masetti R, Fagherazzi S, Montanari A (2008) Application of a barrier island translation model to the millennial-scale evolution of Sand Key, Florida. *Cont Shelf Res* 28:1116–1126
- McCall RT, Thiel V, de Vries JSM, Plant NG, Van Dongeren AR, Roelvink JA, Thompson DM, Reniers AJHM (2010) Two dimensional time dependent hurricane overwash and erosion modelling at Santa Rosa Island. *Coast Eng* 57:668–683
- Meyer M, Harff J, Gogina M, Barthel A (2008) Coastline changes of the Darss-Zingst peninsula—a modeling approach. *J Mar Syst* 74:S147–S154
- Muller A (2001) Late- and Postglacial sea level change and paleoenvironment in the Oder estuary, southern Baltic Sea. *Quatern Res* 55(1):86–96
- Oey LY (2005) A wetting and drying scheme for POM. *Ocean Model* 9:133–150
- Otto T (1913) *Der Darss und Zingst: Ein Beitrag zur Entwicklungsgeschichte der vorpommerschen küste*. *Jahresber-Geography-Gesells Greifswald* 13:237–485
- Roelvink JA (2006) Coastal morphodynamic evolution techniques. *Coast Eng* 53:277–287
- Roelvink JA, Reniers AD, van Dongeren AP, van Thiel de VJ, McCall R, Lescinski J (2009) Modelling storm impacts on beaches, dunes and barrier islands. *Coast Eng* 56(11–12):1133–1152
- Schiewer U (2008) Chapter 2: The Baltic coastal zones. In: Schiewer U (ed) *Ecology of Baltic coastal waters*. Springer, Berlin. doi:10.1007/978-3-540-73524-3
- Schumacher W (2002) Coastal evolution of the Darss Peninsula. *Greifswald Geogr Arb* 27(D2):165–168
- Schumacher W, Bayerl KA (1999) The shoreline displacement curve of Rügen Island (Southern Baltic Sea). *Quatern Int* 56:107–113
- Schwab DJ, Bennett JR, Liu PC, Donelan MA (1984) Application of a simple numerical wave prediction model to lake Erie. *J Geophys Res* 89:3586–3592
- Schwarzer ML (1973) Barrier Islands. *Benchmark Papers in Geology (series)*. Dowden, Hutchinson, and Ross, Stroudsburg, 451p
- Schwarzer K, Dising M (2003) Coastline evolution at different time scales - examples from the Pomeranian Bight, southern Baltic Sea. *Mar Geol* 194:79–101
- Seifert T, Fennel W, Kuhrts C (2009) High resolution model studies of transport of sedimentary material in the south-western Baltic. *J Mar Syst* 75:382–396
- Smagorinsky J (1963) General circulation experiments with the primitive equations, I, The basic experiment. *Mon Weather Rev* 91:99–164
- Rostock S (1994) *Generalplan Küsten-und Hochwasserschutz Mecklenburg-Vorpommern*. Landesentwicklung und Umwelt Mecklenburg-Vorpommern, Ministerium für Bau, 108 pp
- Sunamura T (1992) *Geomorphology of rocky coasts*. Wiley, Chichester
- van Rijn LC, Nieuwjaar MWC, vanderKaay T, Nap E, von Kampen A (1993) Transport of fine sands by currents and waves. *ASCE J Hydraul Eng* 119:123–143
- von Storch H, Langenberg H, Feser F (2000) A spectral nudging technique for dynamical downscaling purposes. *Mon Weather Rev* 128:3664–3673
- Weisse R, Hv S, Callies U, Chrastansky A, Feser F, Grabemann I, Guenther H, Pluess A, Stoye T, Tellkamp J, Winterfeldt J, Woth K (2009) Regional meteo-marine reanalyses and climate change projections: Results for Northern Europe and potentials for coastal and offshore applications. *Bull Am Meteorol Soc* 90:849–860
- Wu CY, Bao Y, Ren J, Shi HY (2006) A numerical simulation and morphodynamic analysis on the evolution of the Zhujiang River Delta in China: 6000~2500 a BP. *Acta Oceanol Sin* 28(4):64–80
- Wu CY, Ren J, Bao Y, LEI YP, Shi HY, He ZG (2007) A long-term hybrid morphological modelling study on the evolution of the Pearl River delta, network system and estuarine bays since 6000 aBP. In: Harff J, Hay WW, Tetzlaff DM (eds.) *Coastline Changes: Interrelation of Climate and Geological Processes*. The Geological Society of America, Special Paper 426:199–214
- Zhang WY, Harff J, Schneider R, Wu CY (2010a) A multi-scale centennial morphodynamic model for the southern Baltic coast. *J Coast Res*. doi:10.2112/jcoastres-d-10-00055.1